



While **SAFEX International** selects the authors of articles in this Newsletter with care, the views expressed are those of the authors and do not necessarily represent the official position of **SAFEX International**. Furthermore, the authors and **SAFEX International** cannot accept any liability for consequences arising (whether directly or indirectly) from the use of any advice given or opinions expressed in this Newsletter

CONTENTS

| | |
|---|----|
| Message from our Chairman | 1 |
| From the Secretary General's Desk | 2 |
| Forthcoming International Conferences | 4 |
| Reaction Sequences Leading to Explosion/ Detonation | 4 |
| Neutralization of Explosives by a Chemical Reduction Product | 7 |
| Explosives Assisting with Safety and Security | 11 |
| Characterizing the Energy output generated by a standard Electric Detonator using Shadowgraph Im- aging | 13 |
| Danish experiences with obtaining regulatory ap- proval for explosives storage facilities | 25 |
| Tony's Tale Piece | 30 |

MESSAGE FROM OUR CHAIRMAN -JOHN RATHBUN

Reflections December 2016

From the seat of the Chairman of SAFEX I have two main perspectives. One is the more pleasing one in that the health of the organization is strong. Today, SAFEX enjoys a strong membership that numbers 76 distinct paying members with a total of 276 different companies from countries that cover the globe! Companies that were never within the reach of the organization in the past, today are receiving



newsletters, incident reports, incident investigation reports, access to e-learning and industry experts! All with the hope and understanding that their company is learning from each one of us and we are making our industry safer. In addition to all this, we are also sound financially from the fiscal prudence of past and current leadership. From these perspectives, I would say that SAFEX has never been better. Thank you all.

However, from another perspective, I see the organization challenged to make a meaningful impact in today's world. We struggle to receive incident investigation reports from our membership. In 2016 we received a grand total of 13 incident reports and a total of 4 investigative reports. As an industry, we continue to see emulsion pump explosions, we fail to see risk patterns and share learnings (i.e. the recent spate of shock tube plant detonations) and we are losing our most educated, prepared, serious colleagues annually to retirement or downsizing. It is truly concerning and we all need to take not just notice but initiate some degree of action.



CONGRESS XIX

NEXT CONGRESS
15-20 May 2017 at the
Scandic Grand Marina
Hotel

How can we do this? We need to elevate the importance of genuine safety awareness within each of our organizations. All of us. At all levels of each member organization. It is up to each one of us. We need to manage in all directions. Horizontally with peers and colleagues. Vertically up and down the chain of command. Everyone needs to not just nod their head and say the right words, we need to get everyone to behave and act in responsible and safe ways. We need to learn from others and audit ourselves.

If we believe that we want to work within safety oriented organizations and to protect lives, then we should find ways to share the information with the industry that is being generated when an event occurs. We should lobby to those senior managers within the member companies, who are the decision makers that we need to do deep-dive investigations that reveal our shortcomings as managers and allow us to improve to prevent a similar event from happening again and to share with other companies the lessons learned. This is the spirit of what the founders of SAFEX wanted to achieve with the organization when it was founded 60+ years ago - and indeed was very successful as has been shown by the progress that SAFEX and the industry made in subsequent years. Sadly that period of enthusiasm and commitment seems to have passed.

FROM THE SECRETARY GENERAL'S DESK

The content of the letter from our Chairman, John Rathbun, is of critical importance to SAFEX and the safe future of our industry. As John rightly said there were 13 Incident reports in 2016 of which 3 recorded fatalities. Most of these were probably preventable through learning and sharing of Incident Reports and Notices -**the latter an obligation you agreed to when you signed up as a member. I urge you to submit the final reports – we have less than 5% being submitted to SAFEX.**

| Incident Notice | Incident Type | Country | Member |
|-----------------|--------------------------|--------------|----------------------|
| 01-16 | HMX/Al Powder Explosion | South Africa | AEL |
| 02-16 | Nitrocotton Fire | Spain | MAXAM |
| 03-16 | Flare Composition Fire | USA | Chemring |
| 04-16 | HMX/Al Powder deflagra- | Russia | AZOT |
| 05-16 | Flare Composition Fire | Australia | Chemring |
| 06-16 | Storm Damage to PETN | Argentina | Austin |
| 07-16 | Detonator Explosion | USA | MAXAM |
| 08-16 | Cap Explosion | Australia | Australian Munitions |
| 09-16 | RDX Detonation | Australia | Australian Munitions |
| 10-16 | Gear Pump Explosion | Chile | Orica |
| 11-16 | Packaged Plant Explosion | Chile | Orica |
| 12-16 | Lead Azide Explosion | Brazil | MAXAM |
| 13-16 | Truck Incident | Costa Rica | Austin |

At the upcoming Congress during May 2017 in Helsinki one of the objectives of all the participants will be to forward ideas to the Board of Governors on how do we as an industry move forward towards being the safest industry in the world and what should SAFEX's role in this be. I look forward to your inputs to make SAFEX the best and oldest industry body on the Globe!

During the last 3 months the eLearning module has moved rapidly forward with the Spanish translation off the BoS module being launched. The Russian translation is progressing well and we target the next module : **Incident Investigation** to be

completed by the end of April 2017 .All these are available tools to ensure better trained and experienced employees that will ensure safe operations .

It is with regret that the Board of Governors had to accept Enrique Barraincúa’s resignation from the Board .Enrique did most of the work on the BoS Spanish translation and SAFEX and the industry thank him for doing this important work .Enrique asked that I place his farewell note :

“SAFEX is an organization with the ultimate goal of saving lives and that common purpose is the bond that holds us all together, in spite of the fact that we may belong to different companies. As long as we continue sharing our experiences, we will help the industry become a safer place in which to work and because of that we should be proud.

For the last eight years I have had the privilege of serving on the Board of Governors, from which I have recently resigned, due to some changes in my professional activities. It is not without pity that I say goodbye to its members, current and former, with whom I have worked all this time. I can say that it has undoubtedly been a rewarding and pleasant experience.

I am thankful for their support and understanding and I do hope to keep on meeting them often, starting with our forthcoming Congress to be held next year in Helsinki, where I also hope to see as many Delegates as possible.

See you soon!”

Andrea Sánchez Krellenberg replaces Enrique on the Board of Governors as the MAXAM and Europe representative.

Andrea holds a Bachelor’s Degree in Chemical Engineering from the Universidad Central de Barcelona and an Executive Development Program from IESE Business School.

Before joining MAXAM, Andrea has developed her professional career in Du Pont where she performed management functions within the areas of H&S, Operations and Consulting, working for different Business units.

She also worked as an EMEA Solutions Architect Cultural Change & Transformation, before joining MAXAM. She managed international consultancy projects and supported companies to improve their Safety Performance in the Workplace Safety and Process Safety. This was done in various industry sectors:

- Chemical
- Petrochemical
- Paper
- Paint



We welcome Andrea to the team and look forward to her valuable input over the next few years.

The Registration Forms for the XIX Congress has been sent out to everybody– thank you for those who already registered ,remember registration closes on 20 February ,so let me have your completed form as quickly as possible as there will be a limit to the numbers we can accommodate .Also ensure early reservation of your room at the Scandic Grand Marina in Helsinki!

FORTHCOMING INTERNATIONAL CONFERENCES

ISEE to be held in Orlando , Florida from 29 till 1 February 2017. Contact: www.isee.org

The 8th Conference and Workshop on Explosives Education and Certification of Skills to be held in Arlanda, Sweden from 13 till 14 June 2017. Contact : erik.nilsson@kcem.se

EFE 9th World Conference on Explosives and Blasting, to be held in Stockholm, Sweden from 10 till 12 September 2017. Contact: info@efee2017.com

Reaction sequences leading to Explosion/Detonation

By

S.K. (Jim) Chan

Condensed explosives possess very high potential energy densities. Commercial explosive such as ANFO has a heat of detonation of 3.2 MJ/kg while military explosives have much higher values, e.g. 5.9 MJ/kg for TNT. In its normal use, the explosive charge is detonated to generate very high pressure to perform work on the surrounding material, such as rock around a bore-hole. At a density of 820 kg/m³, ANFO has a detonation pressure of 4.7 GPa. Of course this pressure is the theoretical peak value (Chapman-Jouguet or CJ) behind the detonation wave for an infinite diameter charge. The actual value in practical applications would depend on the diameter and the compressibility of the confinement material. If the energy is released uniformly in a fixed volume, the pressure is lower at 2.14 GPa, or about half the CJ value but it is constant throughout the entire volume. This is called the explosion pressure of the explosive and is independent of the charge dimensions. In an accident, the energy released is much less than the ideal value due to less than ideal conditions needed for complete reaction of the ingredients. Nevertheless, even a fraction of the energy is sufficient to cause tremendous amount of damages to the surroundings. This fact is the major reason for the use of explosives in e.g. rock breaking, warfare etc. On the other hand, the consequences resulting from an accidental explosion or detonation of a large amount of explosive during manufacturing and handling is also obvious. The sustained operation of any explosive manufacturer must depend on how well it can prevent frequent occurrence of accidents involving explosives.

In an explosive event, normally only the resulting damages caused by the high pressure gas products can be seen. However, if the event is recorded with a high speed camera then it would have reviewed a sequence of exothermic chemical reactions in different formats generating high pressure and high temperature gases in ever faster speeds. Broadly speaking there are three categories of explosive reaction forms: combustion, thermal explosion and detonation. Detonation is a supersonic reaction wave propagating through the explosive mass with a leading high pressure shock front. Combustion is a chemical reaction front propagating through the explosive at a subsonic speed that increases with pressure. Both detonation and combustion possess a wave structure, with increasing temperature behind the wave front as a result of the chemical reaction, despite the highly different wave velocity. Thermal explosion happens when the explosive mass is subjected to an external heat source that heats the internal volume slowly causing the entire mass to warm up almost uniformly up to the ignition point. Subsequently the entire mass would react almost simultaneously. One should realize that all three chemical reaction forms are initiated thermally. In the case of detonation, the leading shock front compresses the explosive to high temperature either in the bulk of the explosive mass, at very high detonation velocities, or in local hot spots, at lower detonation velocities. In the case of combustion, heat is transmitted from the high temperature part at the rear end of the reaction wave backward to the fresh material entering the wave, heating it to the ignition point.

Explosives, with the exception of primary explosives such as lead azide etc., can only detonate if it is subjected to a high pressure shock wave induced by either the detonation of an adjacent mass of explosive, e.g. a detonator, the impact by a high velocity object or through a deflagration-to-detonation transition (DDT) process. A DDT process starts with the combustion of the explosive that generates high pressure waves in a confined volume. If the column of explosive is sufficiently long the pressure waves can coalesce forming a high pressure shock front. When the shock pressure increases to a sufficiently high value fast chemical reaction can be initiated leading to the detonation in the remaining explosive mass. In normal operations of explosive manufacturing and handling, one should not encounter conditions that generate high pressure shock waves. Therefore, in almost all explosive incidents the origins can be traced to thermal ignitions by local energy input sources. Accidents are

related to confined combustion leading to an explosion, thermal explosion or detonation via DDT.

The traditional means of hazard prevention was based on “experience” that was a purely empirical approach demanding strict adherence to rules and detailed operation procedures of a specific manufacturing process. Unfortunately, experiences cannot be applied to new explosive formulations or to modern highly efficient manufacturing processes and machineries. In modern explosive operations, prevention of accidental explosion/detonation must depend on the manufacturer’s ability to predict the ignition sources and to avoid them by mitigation techniques applied to the design and operation of the manufacturing processes. Some explosive manufacturers, such as Orica, use quantitative hazard quantification methods to design and analyze all explosive manufacturing machineries and processes. These methods apply quantitative experimental techniques (Refs.1,2) to define the ignition probability from potential heat input sources. Typical heat sources (Ref.1) include the following: instantaneous friction, continuous friction, low velocity impact (solids and liquids), high velocity (shock wave source), fast heating high temperature sources, slow heating low temperature source, electrostatic, etc. Thermal ignition depends strongly on the temperature, heating rate of the source and the dimension and physical thermal characteristics of the explosive. It is almost impossible to use one single test to cover all possibilities of purely thermal events. Fortunately, one can often predict the ignition conditions with theory for zero or first order reaction kinetics, provided the reaction rate parameters, e.g. activation energy and frequency factor, are known. Therefore, it is important to design experiments to measure the reaction rate parameters (Ref.3) to allow the use of theories to predict purely thermal ignitions.

If the source of ignition is sufficiently energetic, the explosive can be ignited. Here ignition is defined as the condition when the explosive will undergo exothermic chemical reaction producing more energy than that from the input source to allow a self sustained reaction in the form of combustion of the explosive material. What happens next will depend on many external factors as shown in Fig.1. Combustion can only progress in a self-sustained manner if the pressure is above the Minimum Burning Pressure or MBP (Refs. 1,3,4). The MBP can be used as a maximum value to limit the process pressure to prevent accidentally produced local heat sources from initiating burning in the explosive mass. Once burning occurs, the reaction gas products generate high pressure in a confined volume leading to an explosion, or worst detonation through the DDT process, of the vessel. The relatively high MBP values

(Ref. 4) are the reasons that simple mixing of modern commercial explosives does not allow it to burn in an open vessel that can result in significant explosive events. However, high speed mixing, e.g. in a pin mill, is a different matter. In this case, the high shear between the pins, let alone any deformation of the pins, can produce continuous heating of the explosive. Excessive mixing in these machines increases the explosive temperature continuously vaporizing its water content. The characteristics of the explosive will be changed including a reduction of its MBP. Further operation of the machine on the explosive will increase its temperature until it reaches the ignition conditions to start burning ending in the explosion of the entire vessel.

When the processing pressure is higher than the MBP, even if the explosive starts to burn, an explosion may not occur if the strength of the vessel is low such that the pressure is vented by rupturing of the vessel releasing the pressure harmlessly. In fact, it has been shown (Ref.5) that conventional rupture disc can be used effectively for this purpose to quench incipient chemical reactions to prevent subsequent combustion leading to an explosion. Indeed, high pressure pumps are equipped with rupture discs by some manufacturers for this purpose. Unfortunately, rupture discs are only effective in pumps with a continuous path connecting all parts of the explosive inside that allows the pressure to be vented quickly. Pumps such as progressive cavity designs are not suitable for use with rupture discs since the explosive inside the pump is divided into separate volumes that are almost isolated from one another.

If the rupture strength of the vessel is higher than the MBP of the explosive, a self-sustained combustion of the explosive can propagate from an ignition source generating hot gases to increase the pressure inside the vessel. If this happens, the combustion will continue with ever increasing rate, due to the increase in linear burn rate with pressure and the geometrically increase in burning surface area, until one of the following two events happens. The first possible event is when the internal pressure exceeds the vessel wall strength resulting in the explosion of the vessel producing high velocity wall fragments and high pressure air shock, both of which can cause damages to the surrounding. The second possible event is the worst case scenario of a detonation of the entire mass of the explosive in the container if the vessel is sufficiently long to allow DDT to occur.

Experiments at Orica showed that DDT is extremely unlikely to happen in most modern commercial explosives, such as emulsions, that are sensitized by air bubbles or other compressible media used to reduce the density of the explosive. At typical MBP’s less than 5 MPa for small diameter emulsions, the explosive is compressed to higher densities that render the explosive critical diameter to exceed the dimensions of the pressure vessel. An exception is the example of progressive cavity pumps quoted above. In these pumps, if an explosion occurs in one high pressure cavity, high pressure shock can propagate, e.g. through the gaps between the contacting surfaces of the rotor and the body, to the cavities containing the lower density explosive or even back to the source of

fresh material at the pump inlet. Accidents in this kind of pumps happened a number of times in the past. The reasons of most of these accidents were traced to dead-head pumping where the operator closed the exhaust valve without stopping the pump. The continuous frictional energy can cause the following to happen. Firstly the explosive will heat up from absorbing the pump energy. Secondly, the characteristics of the explosive will change, such as water vaporization creating vapor bubbles, which can lower the MBP and increase the sensitivity of the explosive. If the pump continues running then it is a matter of time before the temperature in some part of the explosive will reach a threshold value that ignites the explosive followed by disastrous consequences of pump explosion or detonating of the entire container of fresh explosive at the inlet.

From the above descriptions, it is realized that modern water containing explosives, e.g. emulsions or water gels, that do not contain sensitive chemical ingredients, have MBP's well above atmospheric. They are therefore intrinsically safe in handling and processing operations at low or near atmospheric pressure. These new formulations are indeed a quantum step improvement in processing safety over the old ones containing nitroglycerine. Nevertheless, in the design of processing equipment and operating procedures, one must still have an appreciation of the fundamental safety characteristics of these explosives and the manner under which an explosive event can occur. Lastly, we should also realize that the state of the explosive can change under external conditions that will change its safety characteristics. One example is the explosive under dead-head pumping described above. Another example is solid ammonium nitrate (AN) subjected to external fire. The solid AN can be liquefied by the heat of the fire and the liquid temperature will increase until it starts to decompose producing gas vapour bubbles in the liquid. The detonation sensitivity of liquid AN is significantly increased with the presence of gas bubbles and the high temperature above its decomposition point of 210°C. The presence of gas bubbles also reduces the thermal conductivity of the liquid AN significantly. This factor reduces the critical dimension to initiate a thermal explosion at the same material temperature. Data in Ref.6 shows that the critical diameter of molten AN at a density of 0.8 g/cc is 38 mm (compared to about 500 mm for prilled AN at the same density, Ref.7) and the critical impact initiation velocity with a 50 mm diameter projectile is 190 m/s. The latter is a very low velocity and can be easily generated by the explosion of a metal container, e.g. fire extinguisher present in most trucks. Future studies with the latest knowledge, experimental and modelling methodologies will improve our understanding in this important area.

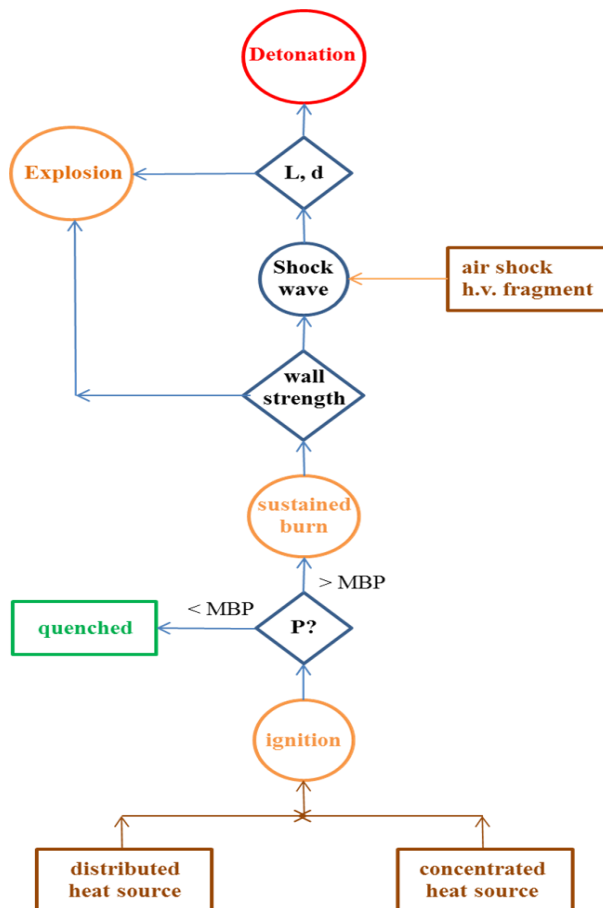


Fig.1 Schematics of reaction sequence leading to an explosive event.

References

1. Chan, S.K., Quantitative hazard testing techniques for water-based explosives, International Symposium on Pyrotechnics and Explosives, Beijing, October 12-15, 1987.
2. Chan, S.K. and Turcotte, R., Probit analysis of friction sensitivity of explosives, 35th International Pyrotechnics Seminar, Fort Collins, Co., July 13-18 (2008).
3. Chan, S.K. and Kirchnerova, J., "Ignition and combustion characteristics of water-gel explosives," U.S. DOD 18th Explosives Safety Seminar, Sept.12-14, San Antonio, Texas, 1978.
4. Chan, S.K. and Turcotte, R., "Empirical correlation of minimum burning pressures of emulsions", 2016, Propellants, Explosives, Pyrotechnics, Vol.41, No.2, pp.207-211.
5. Chan, S.K. and Deshaies, R. "Rupture Disc Pressure Release for Confined Ignition of Condensed Explosives", Propellants, Explosives and Pyrotechnics, Vol.13, No.1, pp.1-7, Feb.1988.
6. Bauer, A., Heater, R.D. and Paterson, J.H., "The sensitivity of ammonium nitrate melts and solutions to projectile impact", Oct. 1981, The Department of Mining Engineering, Queen's University, Kingston, Ontario, Canada.
7. King, A. Bauer, A. and Heater, R.D., "The explosion hazards of ammonium nitrate and ammonium nitrate-based fertilizer compositions, A Summary", Oct. 1982, The Department of Mining Engineering, Queen's University, Kingston, Ontario, Canada.

Neutralization of Explosives by a Chemical Reduction Product

By Valentine A. Nzungu, PhD

CEO and Chief Technology Officer

MuniRem Environmental, LLC

Introduction

Militarization, demilitarization and commercial explosives manufacturing activities generate diverse explosives contaminated media, including bulk explosives, explosives contaminated buildings, equipment, personal protective equipment (PPE), scrap metal, wastewater, sludge and soil. The most common “first generation” disposal of energetic materials (EM) and energetic material contaminated wastes (EMCW) continues to be by open burning and open detonation (OB/OD). Incineration, a “second generation” method is also applied, but is currently enjoying unfavorable regulatory and public acceptance. A “third generation” of methods including; cryogenic cutting, supercritical CO₂ extraction, hydrothermal oxidation, biodegradation, and electrochemical treatment have been developed and are applied. A “fourth generation” method is a non-thermal destruction method that uses chemistry to achieve instant or near instant neutralization and destruction of explosive compounds to innocuous end-products.

The OB/OD of explosive is perhaps the most common and preferred solution for disposal of explosives in use worldwide. The current unfavorable regulatory and public acceptance of OB/OD methods of explosives and explosive waste disposal continues to grow. The public is demanding that regulators ban all permitted OB/OD disposal practices. The opposition to OB/OD methods is fueled in part by the growing volume of data showing that this common practice does not achieve complete destruction of the explosive compounds and forms hazardous end products. The undestroyed parent explosive and incompletely degraded compounds have been shown to be harmful to human health and the environment. Additionally, the cleanup of OB and OD sites takes decades and is quite expensive. There is therefore an immediate and growing need for alternative technologies to replace some OB/OD practices.

Since organic explosives and chemical warfare agents are generally oxidized organic compounds, they are susceptible to biotic and abiotic oxidation or reduction reactions. As a result, a number of developed chemical methods now show promise as alternatives for the neutralization and destruction of explosives. One of such methods is MuniRem; a reagent that applies reduction chemistry to rapidly destroy organic and inorganic explosives to innocuous end-products.

An Innovative Solution for Chemical Neutralization of Explosives

MuniRem[®] is a successfully demonstrated chemical reduction process for explosives (e.g., RDX, HMX, TNT, DNT, ANDTs, picrate, black powder, trinitroresorcinol, Lead styphnate, TNB, and NG), and for remediation of chlorinated organics and metals. The MuniRem[®] chemical reagent consists of selected sulfur bulk reductants uniquely formulated to catalyze near instant neutralization of bulk explosives and rapid destruction of explosive residuals in different materials. The formulation generally contains hydrosulfite and MuniRem[®] proprietary compounds, including sodium salts, carbonate salts, mineral acid derivatives, and a carboxylic acid derivative.

When the MuniRem reagent is applied to contaminated soil and/or munitions debris and water is added, it generates free radicals that react very rapidly to completely degrade oxidized organic compounds, such as explosives into non hazardous, non-energetic end-products. The identified end products of explosives degradation by MuniRem are primarily formate, carbon dioxide, small quantities of oxalate and acetate, nitrite, nitrogen gas, and nitrous oxide gas (only detected in laboratory bench-scale tests). Dissolved metals are precipitated as insoluble sulfides and rendered non-bioavailable. Unreacted MuniRem degrades into innocuous end-products. MuniRem is a new product and is continually finding wider industry applications. The process of matching the MuniRem chemical to the situation and achieving complete neutralization of the explosive hazard has been successfully demonstrated many times.



Figure 1. MuniRem[®] reagent is packaged and shipped in DOT approved containers.

Case Study #1: Decontamination of H-6 Explosives Contaminated Equipment and Building Fixtures

An international ammunition manufacturer required a solution for the safe cleaning and removal of equipment from a building. H-6 (1.1D) explosives contamination was present in bulk and residual form within the Melter/Flaker machine and building fixtures. H6 is a military explosive composed of the following: 44.0% RDX and Nitrocellulose, 29.5% TNT, 21.0% powdered aluminum, 5.0% paraffin wax, 0.5% Calcium Chloride. H6 is relatively sensitive to impact shock and friction, but not as sensitive as many other explosives. It is not as sensitive as RDX. H6 has a melt temperature at about 80°C (176 °F) for TNT and an initiation temperature of between 205 °C and 250 °C (410 to 482 °F) depending on the type of test. RDX has a melt temperature of about 205 °C (401°F). The detonation velocity of H6 is between 7,300 and 7,900 km/sec and it has a TNT equivalency of about 1.35. H6 is not significantly water soluble.



Figure 2. Grate on top of the melter/flaker is covered with H6 and tar pieces and residue is observed in hopper (Photos by Safety Management Services).



Figure 3. Equipment and building fixtures heavily crusted with explosives (Photos by Safety Management Services).

The Melter/Flaker machine was formerly used to recover H-6 (1.1D) explosives during demilitarization operations. Based on sampling of wall surfaces and a visual assessment of the building, it was assumed that 100% of all surfaces within the building were contaminated with H-6 including: ceiling, walls, floors, Melter/Flaker apparatus, fume hood, utility pipes, utility fixtures, conveyor belt with components, work platforms, structural supports tools, miscellaneous debris (brooms, rods, wooden handles, containers), and Melter/Flaker accessory components.

After review of multiple solutions, the client specified the use of MuniRem reagent for safe recovery and chemical destruction of the bulk explosives from the equipment. A field staff consisting of UXO technicians and chemists was assembled to perform the decontamination tasks. Prior to starting any field work, a sufficient quantity of MuniRem reagent in powder form was shipped to the project site. The MuniRem powder was used to prepare MuniRem solution as needed for immediate use. Initial spray application of MuniRem solution was used to desensitize smaller pieces of the H-6 explosives instantly, enabling for safe ingress/egress for intensive recovery of large H-6 chunks. Under a continuous spray of MuniRem solution, the staff removed and transported manageable small batches of H-6 bulk material from hopper and tray assemblies to the nearby process area. This explosive material was then neutralized in reaction tanks containing high strength MuniRem solution.

Although the project plan was based on the assumption that approximately 200 lbs of H-6 was left on the Melter/Flaker unit, over 900 lbs of bulk explosive material was eventually recovered; including over 950 lbs of solids (sludge and sediment). Recovery and neutralization of the bulk H-6 enabled for the safe dismantling of the Melter/Flaker machine, support structures, conveyor assembly, fume hood, ducts and wooden platform with hand tools. The process of cleaning the Melter/Flaker machine with MuniRem produced primary wastestreams of wastewater containing dissolved/neutralized H6 and MuniRem sludge and sediment. Additional derived waste products included soiled cleaning supplies, floor debris and PPE. The generated wastewater (9,550 gallons) was characterized and determined to be non-hazardous; achieving regulatory level compliance in the final disposition of waste streams (liquids and solids) for characteristics of ignitability, corrosivity, reactivity, explosivity, and toxicity. The decontaminated equipment was certified as material determined as safe (MDAS) and shipped offsite for recycling. The project team successfully adapted practices to overcome inclement weather conditions that were unusual for the area: two days of snow, freezing rain, and multiple days with temperatures below freezing.

Case Study #2: Chemical neutralization of multiple explosives: Lead Styphnate, Lead Azide, and Picric Acid

The manufacture of detonators containing high explosives and small arms generates various wastes, including sludge, manufacturing equipment, building fixtures and such other materials contaminated with Lead Styphnate and Lead Azide. Neutralization of Lead Styphnate and Lead Azide by open burning and chemical oxidation are the most commonly applied solutions for the disposal of explosives contaminated materials. Although the explosive hazard is completely removed by open burning, Lead oxide is produced as a hazardous and regulated end product. The Lead tends to leach and pollute soil and groundwater. Thus, by regulatory requirement the ash from the combusted waste must be disposed at a hazardous waste landfill. A more environmentally sustainable solution should simultaneously remove the explosive hazard while immobilizing/stabilizing the Lead as the insoluble metal precipitate.

The results of bench scale treatability tests and multiple full scale applications, have confirmed the efficacy of MuniRem reagent as a solution to rapidly neutralize Lead Styphnate and Lead Azide explosives. The complete destruction of the parent explosives is accompanied by precipitation of the Lead as the insoluble Lead sulfide. The resulting wastewater and solid waste are characterized based on laboratory derived Toxicity Characteristic Leaching Procedure (TCLP) data as non-hazardous waste and disposed as such.

Visually a change in color from yellow to crimson-purple immediately observed when MuniRem contacts Lead Styphnate, ammonium picrate and TNR in the presence of water (Figure 4 & 5). On colored surfaces where the color change may not be easily distinguishable, a piece of white paper dipped into the decontamination solution will indicate if the crimson-purple to yellow-orange color shades have occurred due to the neutralization reactions. To field practitioners, the color change provides the first indication of MuniRem's effectiveness in neutralizing the explosives. Additionally, the instant color change provides a visual guide for the operator to know where explosives contamination and decontamination is occurring as shown in Figure 5. The same rapid and distinct color change is not observed during Lead Azide neutralization with MuniRem.



Figure 4. Instant color change as MuniRem® contacts an aqueous solution of Lead Styphnate

Unlike steam decontamination, the spray application of MuniRem solution on explosives contaminated surfaces destroys the explosives permanently and removes the explosive risk, i.e., renders the treated surfaces safe. When MuniRem is applied to achieve surface decontamination, there is no reappearance of explosive crystals after water has evaporated. The MuniRem solution effectively penetrates cracks and crevices where residual explosives might have accumulated. Injecting MuniRem into pipes and sumps provides a safer and fast approach to neutralize explosives in hard to reach areas during decontamination and routine facility cleanup. In addition to the spray application of MuniRem to decontaminate explosives contaminated surfaces and in different materials, e.g., building pipes, storage and reaction tanks.



Figure 5. Application of MuniRem® to mitigate explosive hazards during demilitarization operations.

MuniRem Environmental has designed and constructed a customized small scale explosive neutralization reactor for bulk explosives destruction to innocuous end products. In a laboratory pilot scale test, a custom designed 100 gallons tanks was used to neutralize multiple batches of 10 pounds of explosives per hour. A neutralization throughput of >200 pounds of bulk explosives per hour is achievable using larger tank reactors with heat exchangers. Application of MuniRem for disposal of recovered bomb fillers can be achieved on site without the need to transfer the energetics to a dedicated facility, thereby avoiding infrastructure capital investment costs for small projects.

For more information on the application of chemical reduction to achieve rapid and safe remediation of explosives and other energetics, please contact Valentine Nzungu at vnzungu@munirem.com or visit our website at www.munirem.com

EXPLOSIVES ASSISTING WITH SAFETY AND SECURITY

Ivo Varga
Senior Technologist
Explosia a. s.
Czech Republic

The company Explosia a.s. is a large manufacturer of industrial explosives, smokeless powders for hunting and sports purposes, rocket motors for rescue systems used in ultra-light aircrafts and explosives for military applications, known not only in the domestic market, but also across its borders.

Although the main products of the company are explosives for mining and quarrying and smokeless powders, it is less known that the company has for more than 20 years worked closely with an integrated rescue system. Of course, cooperation began earlier, for example with analyses of the findings from police actions or firefighters interventions. But after the major floods in the Czech Republic in 1997 and 2002, the need arose for the rapid removal of obstacles in the flow of water, such as fallen trees or broken unmanageable ships.

Special demolition charges were developed by the company Explosia a.s. for these special applications. These demolition charges are based on the Semtex[®] PI SE M plastic explosive, which is a brizant, thermoplastic high explosive. The flagship in the field of special demolition charges are the Semtex[®] RAZORs. Semtex[®] RAZOR is a flexible linear shaped charge capable of cutting various materials by a directed jet of particles. The Semtex[®] RAZOR charges are produced in seven different sizes - 6, 10, 15, 20, 25, 30 and 40 (the number indicates the thickness of steel that the charge can cut through in millimetres). The big charge Semtex[®] RAZOR 40 was, for example, used for sinking of a broken, unmanageable ship on the Labe river during the floods. Nowadays, the annual production of Semtex[®] RAZOR has an annual increase of about 20% and the company holds backup stock for needs of the integrated rescue system.

The family of the Semtex[®] PI SE M demolition charges also includes Semtex[®] PI SE M LCT, breach case BC25 and more recently, disintegrators:

- The abbreviation LCT means, linear cutting tape. These tapes are strips of Semtex[®] PI SE M explosive provided with adhesive layer for better contact with surface. Semtex[®] PI SE M LCTs are made in 4 different sizes - 20, 55, 205 and 740, which means the weight of explosive per one meter of length in grams.
- The breach case BC25 is a compact tool for building barrier breakthrough. The case contains 2.35 kg of explosive with special construction for quick blasting of holes in brick walls. The set includes a supporting foot for the case fixation up to 1.2 m high. The breach case BC25 is capable of breaking a hole of dimensions 1m x 0.5 m through a brick wall 300 mm thick. The breach cases are mainly intended for use in special forces or tactical squads but they can find an application in integrated rescue system.
- Last but not least, there is a new product in portfolio of special charges. Its name is Disintegrator and can be used for disintegration of suspicious bags and subjects. The disintegrator is made in two weights - 13 and 50 grams of explosive. Disintegrator 13 is used for disintegration of suspicious bags and subjects with unsteady case (typically suitcases) at distance of 100 to 800 mm. Impact is made by a fast ($1\,250\text{ m}\cdot\text{s}^{-1}$) substantial cloud with cyclic cut which is slightly expansive. Disintegrator 13 at distance of more than 150 mm commonly do not initiate ANFO, TNT, AN/TNT, RDX/TNT, plastic or emulsion explosives. Disintegrator 50 is used for disintegration of suspicious subjects with thin metal case (steel 1 to 4 mm - typically barrels) at distance 100 to 800 mm. Impact is made the same way like Disintegrator 13. Disintegrator 50 at distance more than 200 mm commonly do not initiate ANFO, TNT, AN/TNT, RDX/TNT, plastic or emulsion explosives.

(Pictures are available on the next page)

The special products portfolio of company Explosia a.s. is broad - more information is available on the company web site www.explosia.cz/en/ -



Examples of using the **Semtex® RAZOR** charges.



Before blasting

After blasting



250 mm

500 mm

750 mm

Distance of disintegrator

Disintegrator 13 and its use.



Plastic sheet explosive **Semtex® PI SE M** and **Semtex® PI SE MLCT** charges.

Foreword

Recently, I had the opportunity to visit the Advanced Explosive Processing Research Group (AXPRO) Laboratory at the Colorado School of Mines. Our team was provided an opportunity to examine product performance at 300,000 frames per second and the outcome was truly astonishing. The ultra-high-speed and shadowgraph imaging technology demonstrated by the AXPRO team offers a remarkable analytical tool of high value to the explosives industry. The following presentation is published with permission from the authors.

J K Shaver, Ph.D.

CHARACTERIZING THE ENERGY OUTPUT GENERATED BY A STANDARD ELECTRIC DETONATOR USING SHADOWGRAPH IMAGING

Vilem Petr. Research Associate Professor and Technical Director of AXPRO, Colorado School of Mines, 1600 Illinois Street, room 120, 80401, Golden, CO. Tel.: +1 303-384-2172. vpetr@mines.edu

Eduardo Lozano. Graduate Research Assistant at AXPRO, Colorado School of Mines, 1600 Illinois Street, room 129, 80401, Golden, CO. Tel.: +1 720-841-0654. jlozanos@mines.edu

Abstract

This research work by the Advanced Explosive Research Processing Group (AXPRO) at the Colorado School of Mines overviews a complete method for the characterization of the explosive energy output from standard electric detonators. This optically-based technique combines high-speed and ultra-high-speed shadowgraph to characterize the casing fragmentation and the detonator-driven shock load. The measurement of the different modes of energy release from standard detonators becomes critical for the device performance evaluation. The procedure here presented could be used as an alternative to current indirect methods - such as the Trauzl lead block test - because of its simplicity, high data accuracy, and minimum demand for test repetition.

This technique was applied to experimentally measure air shock expansion versus time and calculating the blast energy from the detonation of the high explosive charge inside the detonator. Direct measurements of the shock front geometry provide insight into the physics of the initiation buildup. Because of their geometry, standard detonators show an initial ellipsoidal shock expansion that degenerates into a final spherical wave. This non-uniform shape creates varia-

ble blast parameters along the primary blast wave. Additionally, optical measurements are validated using the piezoelectric pressure transducers.

On the other hand, the energy fraction spent in the fragmentation process of the metal casing is obtained using the Gurney model, as well as several empirical formulations for blasts from fragmenting munitions. Due to the particular geometry, the results are further analyzed through a two dimensional numerical model built in AUTODYN 2-D. The fragment size distribution is also studied using particle imaging analysis. Understanding the fragment density distribution plays a critical role when performing hazard evaluation from these types of devices. In general, this technique allows for characterization of the detonator with no knowledge of the amount or type of explosive contained within the shell.

Keywords: High-Speed Imaging, Blast Wave, Fragmentation, AUTODYN, Energy Distribution.

1. Introduction

Presently, standard detonators have two different explosive materials: a sensitive primary explosive (primer charge), and a less sensitive, but more high-powered secondary explosive (base charge). These charges are contained inside a metal cup that is usually made of copper, bronze, or aluminum depending on the application. Upon initiation, the ignition source sets off the primer charge, which detonates the base charge, which in turn detonates the main explosive charge [2]. Depending on the type of energetic material that comprises the main charge, different initiation energy may be required to achieve a reliable detonation.

Conventional detonators are classified according to their strength. The strength is universally represented by a single number that ranges from 1 to 12, which is directly related to the net explosive content of the detonator. The U.S. Bureau of Mines established the number 8 as the industry standard from which important definitions, like "blasting agent," are termed [1]. However, the strength of a detonator is measured not so much by the net explosive weight but by the different tests developed over the years (sand test, Trauzl lead block test, etc.). The reason is because the main factor affecting the performance is the output of the energy release. This output is affected not only by the net explosive weight, but also by the charge geometry, pressing density, casing type and thickness, and even the atmospheric conditions. Hence, it is critical to understand how these parameters affect the generation of the detonator-driven shock load.

High-speed imaging technologies are constantly being improved for the study of detonation properties of explosive materials. Several researchers have reported the use of these technologies from measuring expanding shock waves in the air from bare explosive pellets [3-5]. In addition, Hutchinson demonstrated how the casing surrounding a particular explosive charge can be related to an equivalent bare charge by considering the momentum absorption that takes place during the fragmentation [6].

The goal of this research work was to develop an optically-based experimental method for characterizing the energy

released in terms of fragmentation and explosively driven shock load by a conventional detonator. This technique allows studying the performance of these initiation devices as well as its characterization when its origin is unknown.

2 .Theory Background

A high explosive material is characterized by a detonation process where the front of the chemical reaction moves faster through the material than the speed of sound. This sudden release of energy is usually accompanied by the creation of a propagating disturbance in the surrounding medium known as a shock or blast wave. By knowing the medium and the rate of expansion of this blast wave, one is able to characterize not only the explosive shock load, but also the energy source.

The primary shock front of a blast wave is, in many ways, a determining factor in its behavior [7]. The goal is then to characterize the detonator-driven shock load from its performance in air, which for present purposes may be considered as an ideal gas. According to Needham [8], the ideal gas assumption is accurate at 99 percent for incident blast overpressures up to 2,000 KPa.

Using a Lagrangian coordinate system, the basic parameters in air before and after the pass of the shock wave can be described. Several relations are then obtained for the different blast parameters from the fact that mass, momentum, and energy must be conserved across the shock front. Therefore, shock wave velocity U_s , shock wave Mach number M_s , particle velocity u_s , incident shock wave pressure P_s , etcetera, can be calculated from the sole measurement of the air shock wave expansion rate and the Rankine-Hugoniot relations.

When the primary interest is to study the output of the energy released by an explosive charge, the most reliable method is to measure the distance from the center of the explosion at which a specific blast wave property occurs. This value is then related to the distance at which the same property is produced by a reference explosion using the cube root scaling law [3]. This reference is usually the TNT standard for chemical explosions. On the other hand, conventional detonators have their base charge and components allocated within a light to moderate case. The PV energy available in the explosive charge has to work on the casing before it is able to work on the air. Therefore, the amount of energy given up to the metal is no longer available for the air blast wave [9].

A small fraction of the energy is also expected to be released in other forms such as radiation [3]. The type of detonator referred to in this manuscript is limited to chemical explosive charges. Thus, this energy fraction is expected to be negligible compared to the one associated with the generation and expansion of detonation products.

2.1.Air Shock Characterization

The primary shock wave expansion rate in air from a standard number 8 electric detonator is measured in two directions. The directions correspond with the longitudinal and transverse axes of the detonator. This elliptical expansion of the shock wave is a result of the charge geometry. As the blast wave expands, it decays in strength, lengthens in duration, and slows down, both because of the spatial divergence and because of the medium attenuation [8].

Most of the sources of compiled data for air blast waves from high explosives are limited to bare, spherical charges in free air. However, different experiments conducted with alternative charge geometries show how explosive materials tend to drive their energy to the larger area of their outer surface. This is very important because if the initial expansion wave has a shape different than spherical, the blast parameters will decay at a different rate than that of the reference explosion [9].

Esparza [10] presented a spherical equivalency of cylindrical charges in free air where a higher explosive yield is reached at 90 degrees from the longitudinal charge axis. The difference in the shock wave magnitude in the different directions will decrease as the shock expands through the air, adopting a final spherical shape. This is the case for conventional detonator geometries where the shock travels faster in the transverse direction.

The blast wave expansion rate in atmospheric air is experimentally measured by using retro-reflective shadowgraph. This expansion is obtained along the longitudinal and transverse axes of the detonator providing two sets of data. The measured values are then corrected to Normal Temperature and Pressure (NTP) by using the scaling approach presented by Kleine et al. [3]. The scaling is as follows:

$$R_s = R \left(\frac{P_a}{101.325} \right)^{\frac{1}{3}} \quad (1)$$

$$t_s = t \left(\frac{T_a}{288.16} \right)^{\frac{1}{2}} \left(\frac{P_a}{101.325} \right)^{\frac{1}{3}} \quad (2)$$

The subscript "s" refers to scaled values to NTP conditions. R represents the shock wave radius from the center of the blast and t is the recorded time. P_a and T_a are the ambient pressure and ambient temperature at the time of the experiment. Finally, the shock wave radius versus time in the transverse and longitudinal directions is then fitted to an empirical equation developed by Dewey [11] and reported in references [3] and [4]. This empirical correlation is as follows:

$$R_s(t_s) = A + B a_0 t_s + C \ln(1 + a_0 t_s) + D \sqrt{\ln(1 + a_0 t_s)} \quad (3)$$

where R_s represents scaled shock wave radius from the center of the blast, t_a represents time of arrival of the shock wave, a_0 is the local speed of sound at NTP (340.29 m/s), and A , B , C , and D are the yielding coefficients. B should be set to 1 to guarantee an asymptote to the speed of sound for large times [4]. The calculation

of the parameters A , B , C , and D was performed by least-squares curve-fit through a computational code written in MATLAB®.

A relation between shock wave Mach number versus time can be obtained by differentiation of the Equation (3) and dividing the resulting value by the local speed of sound. This expression is as follows:

$$M_s(t_s) = \frac{1}{a_0} \frac{dR_s(t_s)}{dt_s} = B + \frac{C}{1 + a_0 t_s} + \frac{D}{2(1 + a_0 t_s)\sqrt{\ln(1 + a_0 t_s)}} \quad (4)$$

At this point, an analytical expression for the shock Mach number versus radius is derived for the two main expanding shock directions. The next step will be to quantify the yield of the detonation by the analysis of this shock wave expansion. As previously mentioned, the energy released can be related to that of another reference high explosive of the same mass; in this case TNT [3]. Therefore, the measured shock Mach number versus radius is fitted to the high explosive blast standard. This standard is established for the widely accepted Kingery and Bulmash (K-B) curves [12] for spherical free-air TNT burst. These curves can be obtained from Equations (5) and (6) where T is the common logarithm of the peak shock wave pressure in Pascals.

$$U = -0.214362789151 + 1.350342499937T \quad (5)$$

$$\begin{aligned} Y = & 2.611368669 - 1.69012801396U + 0.00804973591951U^2 \\ & + 0.336743114941U^3 - 0.00516226351334U^4 - 0.0809228619888U^5 \\ & - 0.00478507266747U^6 + 0.00793030472242U^7 + 0.0007684469735U^8 + 1 \end{aligned} \quad (6)$$

Since the data obtained is in terms of shock Mach number, the parameter peak shock wave pressure is converted to shock Mach number using Rankine-Hugoniot relations and the ideal gas assumption ($\gamma = 1.4$). According to Needham [8], the K-B curves provide an accurate representation of the peak blast parameters as a function of the range for ranges greater than about three charge radii. Additionally, the peak blast parameters versus distance for different types of condensed phase explosives are expected to converge for pressure less than approximately 10 bars [8]. A critical aspect must be taken into consideration at this point. The K-B curves are expressed for spherical free-air expanding shocks while the blast waves from conventional detonators will show an ellipsoidal expansion due to their explosive charge geometry (Figure 1).

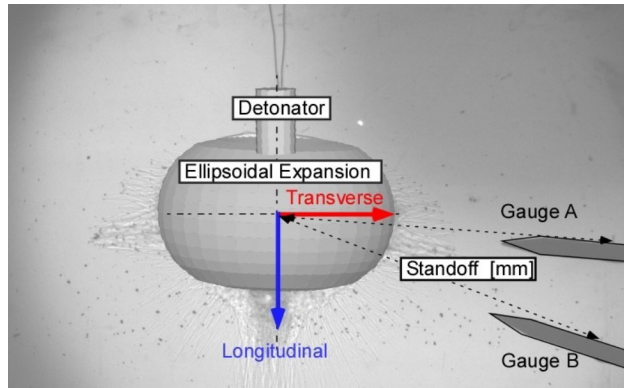


Figure 1. Approximated initial blast wave generated from a standard detonator and axes locations.

This challenge is overcome by applying the basic laws to the blast wave expansion. An equivalent spherical shock wave is then considered by specifying that the volume of air being compressed by the ellipsoidal shock wave is the same as the one compressed by an equivalent sphere of radius R . Next, the equivalent spherical shock wave Mach number versus distance data is fitted to the reference spherical free-air burst yielding a single coefficient. The obtained value represents the equivalent spherical yield of TNT that would produce the measured blast wave properties in atmospheric air. This explosive yield is expected to be lower than the total energy content of the detonator since only the blast wave in air is being accounted for.

It must be mentioned that the classic similar solution for a point energy release and strong shock wave formation by Taylor predicts the motion of the shock wave and the resulting physical property distributions using dimensional analysis [13]. This ideal prediction, however, cannot be directly applied to typical explosions where the energy is released over a finite time. These real explosions are better analyzed experimentally by measuring shock propagation or property variations rather than applying scaling laws [14]. Here, the shock propagation is measured from the center of the explosion as a function of time and becomes the primary data for developing the blast wave characterization in the air.

2.2. Fragmentation Characterization

A significant part of the energy released by a conventional explosive detonator is spent during the fragmentation process of the casing. The energy is transferred to the metal in three modes: shock heating, strain and fracture, and kinetic energy of the fragments [9]. The energy released in the form of a blast wave is thereby reduced, since the expanding explosive product gases will have to spend part of their energy to overcome the strength of the metal shell and accelerate the generated fragments. Hutchinson [6] developed a detailed analysis of the escape of blast from fragmenting munitions, which parts from the physically valid initial assumption provided by Gurney [15].

Three different equations presented in [6] regarding fragmenting casings are compared in order to better estimate the energy partition during the fragmentation. Each equation represents the ratio of the equivalent bare explosive mass to the actual mass as a function of the ratio between the mass of casing and the mass of explosives contained within the casing. The mentioned equations are as follows:

$$\text{Fisher:} \quad C_{EB} = C \left(0.2 + 0.8 / \left(1 + \frac{M}{C} \right) \right) \quad (7)$$

$$\text{Modified Fisher:} \quad C_{EB} = C \left(0.6 + 0.4 / \left(1 + \frac{M}{C} \right) \right) \quad (8)$$

$$\text{Hutchinson:} \quad C_{EB} = C \left(\frac{1}{2} / \left(\frac{1}{2} + \frac{M}{C} \right) \right)^{1/2} \quad (9)$$

where, C is the mass of explosives in the base charge, M represents the mass of the casing surrounding the base explosive charge, and CEB is the equivalent bare charge. Equation (8) is an empirically adjusted version of Equation (7) assuming early fragmentations of the casings while the pressure of the explosive products within them is still high. The explosive products can then escape through the fragmented casing, taking the momentum they would otherwise have to impart to the casing material [6]. However, this modified equation is more representative of brittle casings rather than ductile metals such as the aluminum shell studied in this paper.

Alternative ways for calculating blast impulse reduction due to encased explosive charges has been also studied by Hutchinson [6]. Equation (9) is presented as an alternative to Fisher's formula since the last one does not provide good approximation for $M/C > 5$. Fisher (Equation 7), Modified Fisher (Equation 8), and Hutchinson (Equation 9) are accepted as valid approaches that account for the energy absorption during the fragmentation process. In order to validate the results and applicability of these three formulations (Equations 7 to 9) for this particular experiment, the casing expansion and acceleration will be optically measured using ultra high-speed imaging and correlated to the Gurney model for cylindrical charges:

$$\text{Gurney:} \quad V = \sqrt{2E} \left(\frac{M}{C} + \frac{1}{2} \right)^{-1/2} \quad (10)$$

where, V is the velocity of the accelerated metal, C is the mass of explosives in the base charge, M represents the mass of the casing surrounding the base charge, and $\sqrt{2E}$ is the Gurney constant for the given explosive. By knowing the mass of casing and the casing initial velocity, the absolute mass of explosives contained in the base charge can be calculated and correlated to the values obtained in Equations (7) to (9).

In addition, these results will be further analyzed using a numerical simulation using the hydro-code AUTODYN 2-D and its Smoothed Particle Hydrodynamic (SPH) processor. Equations (7) through (10) consider exclusively the fraction of the energy that is transmitted to the surrounding cylinder of casing. However, part of the explosive energy is exerted on the shell's tip, imparting high velocities to this small area. The results from the numerical model account for that fraction of the energy, improving the overall analysis.

3. Experimental Procedure

3.1. Number 8 Detonator

The detonator studied in this paper is a number 8 mining and construction detonator, the Dyno Nobel's *Electric Super™ SP* [16]. Detonators are designated from number 1 to number 12, with the standard and most extensively used detonator being the number 8.

The detonator studied here can be described as a metal shell that contains a PETN base charge positioned on one end of the shell. Adjacent to this, there is a highly sensitive primer charge housed in a heavy steel sleeve. Next, a fuse head embedded with a bridge wire connects the two leg wires, thus forming a means of electrical ignition. If a firing current is applied to the leg wires, the bridge wire becomes incandescent, and the fuse head is initiated. This initiation sets off the very sensitive primer charge, and subsequently the base charge.

The manufacturer reports a net explosive content of 885 mg of which 555 mg is the PETN base charge. While the primer charge is protected by a relatively heavy steel casing for safety reasons, the secondary explosive base charge is in direct contact with the outer aluminum shell. The aluminum shell has a thickness of 0.42 ± 0.01 mm while the steel sleeve has a thickness of 1.60 ± 0.01 mm. From design alone, it is expected that the air shock will be essentially generated by the lightly cased base charge. This argument will be discussed in the later sections. Figure 2 shows the different components of the electric detonator Dyno Nobel's *Electric Super™ SP* [16].

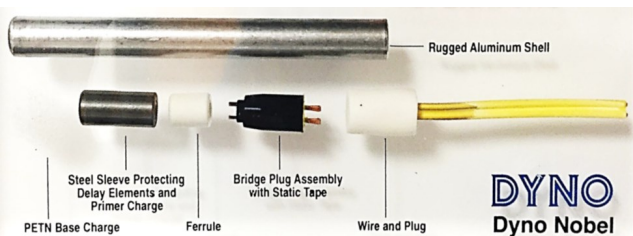


Figure 2. Internal view of a standard electric detonator

3.2. Retro-reflective Shadowgraph Technique

Shadowgraph was invented as a visualization method in 1672, where the Sun was used to cast a shadow on a white surface. Modern shadowgraph differs from this more rustic method in its use of specialized screens, light sources, and high-speed imaging systems. The direct shadowgraph technique only requires a light source, a camera, and a screen on which to create a shadow. The light source is placed at an optimum distance from the screen and from refractive disturbances in the Schlieren object. A shadow is then projected at a certain height onto the screen. The retroreflective shadowgraph, specifically, requires the use of a retro-reflective screen and a rod mirror, which is aligned with the camera axis, illuminating the retro-reflective screen with a significant amount of light, and thus providing a high quality image. This method was introduced by Hargather et al. [17] and is effective for the visualization of blast waves and, in general, any other variation of flow density in the air.

The experimental setup is shown in Figure 3. A high-speed camera, collimated strobe lighting system, lens with a rod mirror, and a retro-reflective screen are required for the execution of the retro-reflective shadowgraph.

The high-speed camera used for blast wave visualization is Vision Research’s Phantom v.711. The ultra-high-speed camera used for the measurements of the casing expansion is Specialized Imaging’s SIM X16. The retro-reflective screen is made of 3M Scotchlite TM 7610, a high gain, industrial grade, exposed-lens, plastic-based material pre-coated with a pressure-sensitive adhesive. The screen used for the experiments is a 2.4 meter square.

3.3. Pressure Gauges

Two PCB Piezotronics model 137A23 pressure sensors were placed in the measurement plane of the camera imaging for the validation of the shock wave parameters measured by optical methods. Both sensors were mounted on a steel stand pointing in an axial direction to the detonator. Standoff distances from the energy source varied from 420 mm to 460 mm. The sensor’s sensitivity is 14.5 mV/KPa ±15% depending on the calibration. The diaphragm was insulated using common black vinyl electrical tape to minimize possible signals generated by flash temperatures, which can result from the passing of the shock front. Additionally, the bodies of the gauges were isolated from the ground by placing common black vinyl electrical tape in contact with the surface of the steel stand.

The two pressure sensors were connected by coaxial cable to a PCB sensor signal conditioner model 482C05. Both outputs were also connected to a Tektronix DPO3014 Oscilloscope where the signal provided by each gauge was recorded. The triggering was implemented from an EIT HB-SBS electric firing system and a digital delay/pulse generator Stanford DG535, which provides a 2-volt output to the lighting system, the high-speed camera, and the oscilloscope.

4. Results and Discussion

4.1. Shadowgraph

A total of nine tests were conducted in air. Tests 1 through 6 were captured using the Phantom v.711 and the goal was to measure the blast wave propagation in different directions. Tests 7 through 9 were recorded using the SIMX16 and the goal was to determine the expansion rate of the detonator’s metal shell. The main cameras’ settings for each individual test are summarized in Table 1.

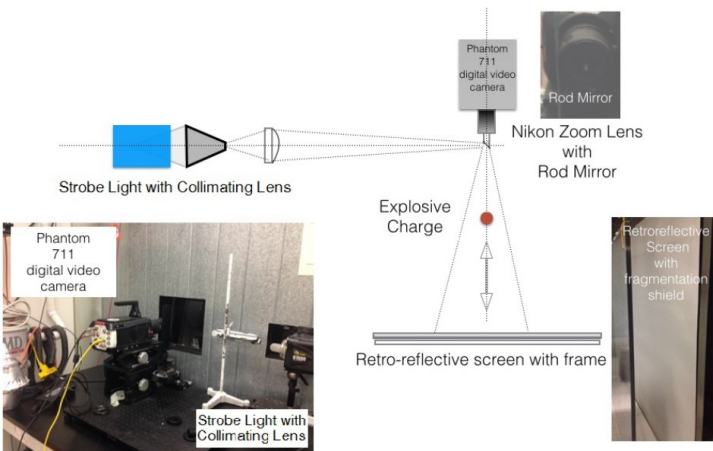


Figure 3. Retro-reflective shadowgraph setup

Table 1. Cameras' settings for each test

| Test | Camera | Resolution | Interframe | Exposure |
|------|---------|------------|--------------|---------------|
| 1 | Phantom | 608x600 | 56 μ s | 0.294 μ s |
| 2 | Phantom | 608x600 | 56 μ s | 0.294 μ s |
| 3 | Phantom | 512x656 | 53 μ s | 0.294 μ s |
| 4 | Phantom | 512x656 | 53 μ s | 0.294 μ s |
| 5 | Phantom | 512x656 | 53 μ s | 0.294 μ s |
| 6 | Phantom | 912x848 | 110 μ s | 0.294 μ s |
| 7 | SIM | 1280x960 | 4.27 μ s | 1.000 μ s |
| 8 | SIM | 1280x960 | 0.27 μ s | 1.000 μ s |
| 9 | SIM | 1280x960 | 0.27 μ s | 1.000 μ s |

Some frame sequences are presented in Figures 4, 5, and 6. As it is shown, the initial blast wave presents a sharp elliptical shape in the two-dimensional plane due to charge geometry. The ellipsoidal shock generated by the explosive charge produces higher shock velocity values in the transverse plane of the charge versus those recorded along the longitudinal axis. As the shock expands, the spatial divergence and medium attenuation cause a gradual change in shape ending as a spherical shock wave.

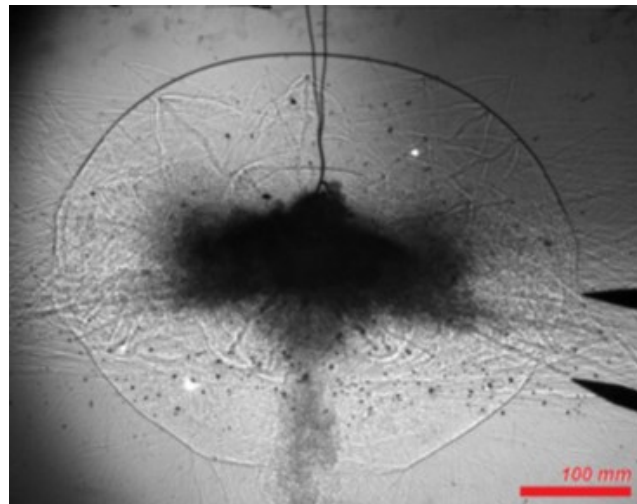


Figure 5. Sample image from test 6 (330 μ s after initiation), the tips of the pressure sensors appear on the right part of the image.

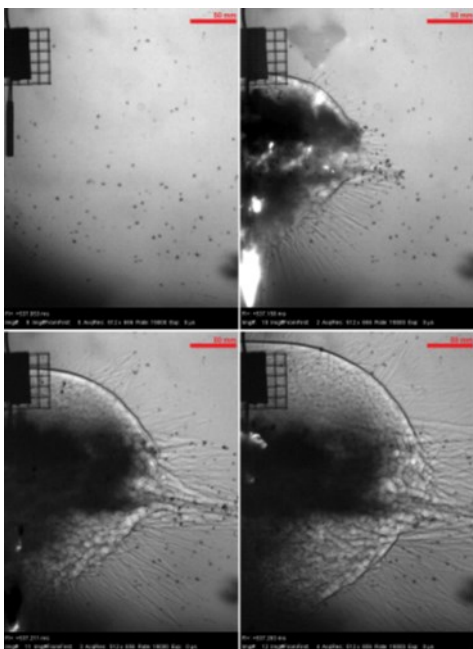


Figure 4. Sample images from test 5, frames are 53 μ s apart

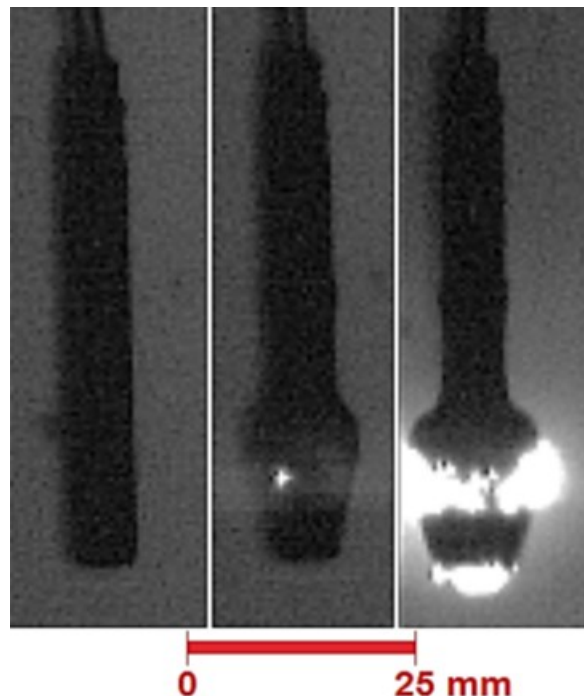


Figure 6. Sample images from test 8, frames are 270 ns apart, the window event is 20 μ s

Figure 6 shows the casing expansion and subsequent fracture during the acceleration process due to the expanding detonation products .

4.2. Gauge measurements

Two piezoelectric pressure transducers were placed in the measurement plane at a distance of 460 mm from the center of the explosion for tests 3 through 6. The top and bottom gauges were placed at - 4° and -20° from the transverse axis of the detonator respectively. The sample length was 10,000 samples with a sample rate set to 500K samples per second. Figure 7 shows the pressure-time signal recorded in test 6 by the top gauge and the smoothed profile.

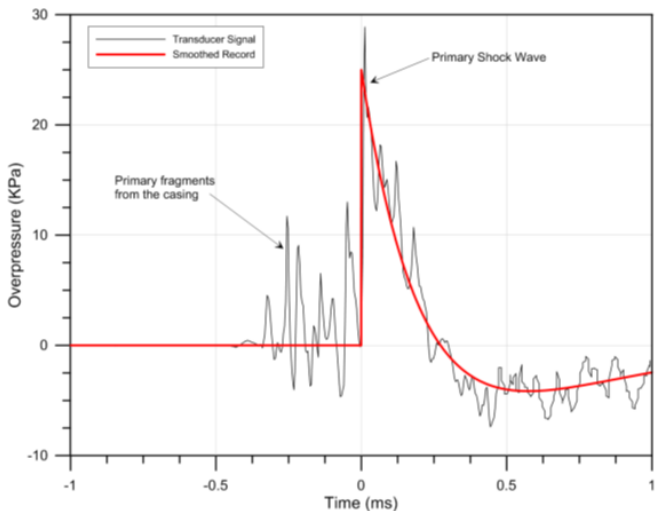


Figure 7. Overpressure-time record (black) and smoothed profile (red) for test 6

The signal is noised during a certain period of time before the shock arrival. This noise is due to the shock waves produced by the primary fragments from the detonator’s aluminum casing as they fly by the transducer’s diaphragm. Some discussion could be made about this noise in the gauge signal. Initially, the experimentalist may think that this noise is attributed to direct fragment impact and subsequent ringing of the gauge fixture. However, a direct fragment impact was observed during the experimentation. Such impact produces a high frequency noise that invalidates the entire record.

Relating to the data analysis, it must also be taken into consideration that the maximum value recorded in the oscilloscope does not match exactly with the peak incident overpressure because of sensor overshoot [18]. In order to obtain the actual peak overpressure, the overpressure-time record must be smoothed. This is done using the analytical methodology presented by Kinney and Graham [7] where peak overpressure, positive duration, and wave form parameter are determined and inserted into the Friedlander equation. In this case, a peak overpressure of 25.02 KPa was obtained for test 6 with a positive duration of 272.5 μs and a wave form parameter of 0.9 (Figure 7). The values obtained for the tests 3, 4, and 5 varied by no more than 0.04 KPa for the peak overpressure.

4.3. Blast Wave Analysis

The shock wave expansion in each direction within a two dimensional plane was experimentally measured for the first six tests. Two directions are recorded corresponding with the longitudinal and transverse axes of the detonator. The same behavior observed for the transverse direction is assumed for the third dimension due to the charge axial symmetry.

From First Principles, it was calculated that the volume of air being compressed by the ellipsoidal shock wave is the same as the one that is compressed by an equivalent sphere of radius *R*, therefore an estimation of the expansion rate for an equivalent spherical shock wave is obtained. This argument seems convenient for explosive yield determination since most of the data from high explosives is presented for spherical charges. As previously mentioned, this initial ellipsoidal blast wave will end up adopting a spherical shape due to geometrical expansion and medium attenuation. Figure 8 compiles the shock wave radius versus time measured in longitudinal and transverse directions, as well as the equivalent sphere for tests 1 through 6. The uncertainty associated with these measurements is ±0.5536 mm due to the resolution of the images.

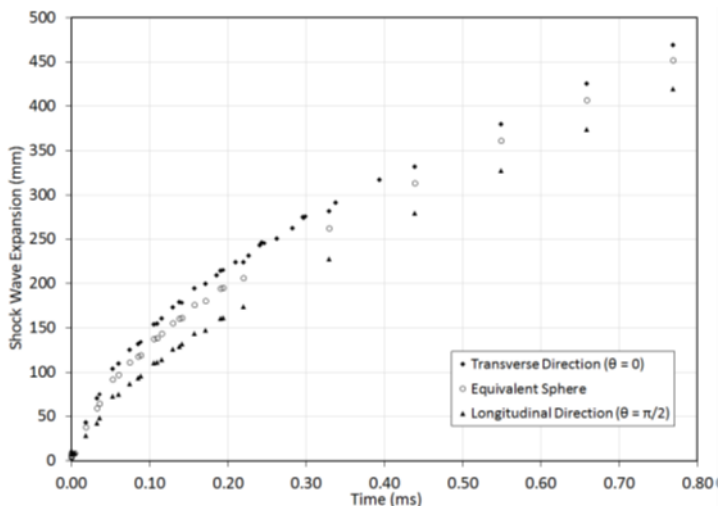


Figure 8. The shock wave expansion rate in transverse direction, longitudinal direction, and equivalent sphere

Shock wave radius and time arrival are scaled using Equations (1) and (2). By applying least-squares regression, coefficients *A*, *B*, *C* and *D* are determined for the use of Dewey’s Equation (3). Table 1 summarizes the obtained fitting coefficients for each direction and the equivalent sphere.

Table 2. Curve fitting coefficients for Dewey’s Equation

| Direction | A | B | C | D |
|--------------|--------|---|---------|---------|
| Transverse | 3.5749 | 1 | 38.8146 | -16.884 |
| Longitudinal | 3.6339 | 1 | 43.305 | -49.641 |
| Equ. Sphere | 3.5961 | 1 | 41.679 | -31.339 |

Although an empirical correlation, Equation (3) does satisfy the appropriate physical condition as the time tends to infinity, ensuring that the shock wave velocity approaches the atmospheric speed of sound. By differentiating Equation (3) and dividing by the local speed of sound, an expression for the shock Mach number versus time is obtained.

From the Rankine-Hugoniot relations, the blast incident overpressure is then calculated in the transversal direction and validated with the data recorded by the pressure gauges. A peak pressure of 25.02 ± 0.04 KPa was recorded by the transducer at 460 mm from the center of the explosion. Conversely, a value of 25.92 KPa is obtained from the shadowgraph measurements. Therefore, a good agreement is observed with a maximum of 7.5 percent difference for the peak overpressure.

The next step will consist of quantifying the energy release by the detonator-driven blast wave. Starting from the Mach number versus time for the equivalent sphere, a relationship between Mach number versus distance can be also achieved. By taking discrete points from this analytical relationship and fitting them to the high explosive blast standard (K-B curves), a single yielding coefficient is retrieved in terms of mass of TNT. The value obtained is 542.67 mg for the number 8 electric detonator studied.

Physically, this mass represents the equivalent sphere of bare TNT that would release the same amount of blast wave energy into the atmospheric air. Figure 9 shows the shock Mach number versus distance from the center of the explosion in the different directions and the equivalent sphere. Kinney et al. [7] also proposed an alternative analytical expression for the calculation of the peak overpressure versus range. This relation is plotted for the obtained 542.67 mg in order to evaluate its accuracy in the gram-scale range.

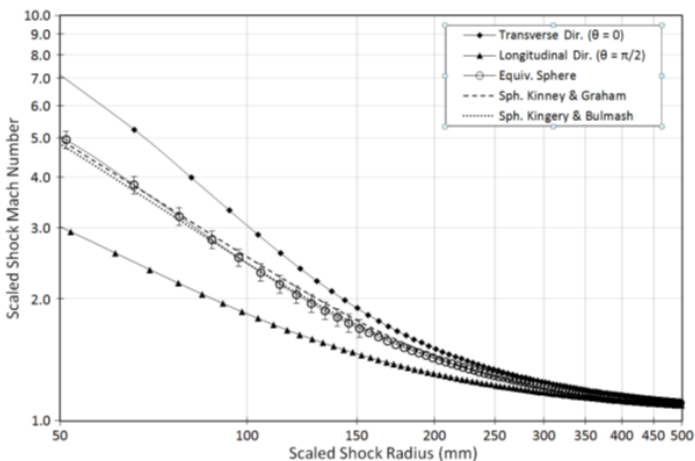


Figure 9. The experimental shock Mach number versus radius in the transverse and longitudinal directional, and fitted reference spherical standard for high explosives

Figure 9 shows good agreement between the measured shock Mach number versus distance and the K-B curve for the obtained yielding coefficient. The data is represented using logarithmic scales starting from a shock radius of 50 millimeters. As previously mentioned,

the reference explosion does not apply well for small radii if the explosives are other than TNT [8]. A maximum 5 percent error is measured between the data provided by the shadowgraph and the high explosives blast reference. This error increases up to 8 percent for the expression provided by Kinney et.al [7]. At this point, the obtained yielding coefficient corresponds to the mass of explosive that actively contributes to the blast wave generation. The next step will be to evaluate the energy partition that goes into the fragmentation of the casing.

4.4. Fragmentation Analysis

In section 2.2, three different equations for cased explosives were presented for the estimation of the momentum absorption of the metal casing. The two magnitudes required for the application of these formulations are the mass of the casing and the equivalent mass of bare explosive. For the calculation of the mass of casing, cylinder length and cylinder thickness are required. The length considered is the one surrounding the explosive base charge. The mass of the casing, 290.07 mg, is obtained from the dimensions of the cylinder metal shell surrounding the explosive charge and the volumetric mass density of the shell. Next, the total explosive mass contained inside the detonator is determined from Equations (7), (8), and (9). Notice the mass will be in terms of the reference explosion, in this case TNT. As it was mentioned in section 3.1, the main difference between Equation (7), Equation (8) and Equation (9) is that the latter considers early fragmentation of the casing.

From the total explosive mass in TNT, the total energy in terms of Kilojoules is calculated by multiplying this term by the heat of detonation for TNT. This value can be obtained from numerous references for different types of explosives within an approximately 3 percent difference. The heat of detonation is the energy release at the Chapman-Jouguet (C-J) condition, and refers to the change in enthalpy. This effective energy developed by an explosive is always less than the assumed thermodynamic energy [19]. In this case, the adopted value for the heat of detonation for TNT is 4,610 KJ/Kg [7]. Table 2 summarizes the energy values in Kilojoules obtained from Equations (7-9)

Table 2. Energy value for bare and cased charge

| Equivalent Bare Charge (KJ) | Mass of Casing (mg) | Cased Explosive Energy (KJ) |
|-----------------------------|---------------------|-----------------------------|
| 2.501 | 290.07 | Eq.(7): 3.260 |
| | | Eq.(8): 2.866 |
| | | Eq.(9): 3.354 |

According to table 2, a percentage difference of up to 16 percent is obtained by the different equations. In order to determine the formulation that best models the energy partition from these types of detonators, further analysis is performed using the Gurney model. From the casing mass and initial velocity, the mass of explosive that accelerates the shell can be obtained using Equation (10). Figure 6 shows different frames of the detonator’s casing expansion and subsequent fragmentation.

The casing expanded 1.494R0 and 1.706R0 in the second and third frames respectively. The uncertainty associated with these measurements is ± 0.178 mm due to the im-

age pixelation. Considering the nominal value obtained, the casing velocity is 2.866 mm/μs. From the velocity and the mass of the casing, Equation (10) yields a total mass of PETN of 532.35 mg and an energy value of 3.319 KJ (considering a heat of detonation for PETN of 6,235 KJ/Kg [19]). This value is 4.08 percent lower than the actual mass of PETN. This error is primarily attributed to the main premise of the Gurney model, which considers the fragmentation process with no losses. That is, the explosive gases can drive the metal for a large portion of the gas expansion [20]. However, the metal casing will fracture at a certain expansion ratio and the acceleration process stops. Since aluminum has a relatively high ultimate strain, the difference obtained is not worse than 4.08 percent.

The explosive energy obtained from the Gurney model lies between the values obtained from Equations (7) and Equation (9) showing that Fisher and Hutchinson equations provide a good estimation for gram-scale cased explosive charges. A significantly lower energy value is obtained from Modified Fisher (Equation (8)) due to the high ultimate strain of the aluminum casing. However, as mentioned in section 2.2, Equations (7) through (10) consider exclusively the fraction of the energy that is transmitted to the surrounding cylinder of casing. Part of the explosive energy is exerted on the shell's tip, imparting high velocities to this small area. In order to evaluate the energy transmitted to that region, a numerical simulation is built in AUTODYN 2-D using the SPH solver. Figure 10 shows the absolute velocity contour at different times during the simulation. The particle size used for the PETN and the aluminum is 0.01 mm.

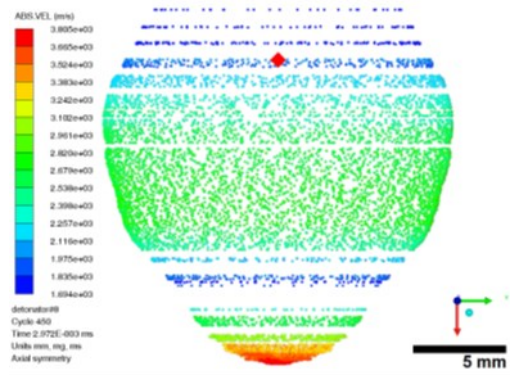


Figure 10. Detonator casing expansion; the red diamond represents the detonation point; particle size is set to 0.01mm

According to the last velocity contour shown in Figure 10, a radial velocity of about 2,900 m/s is achieved at 90 degrees from the detonator's longitudinal axis. This value is in good agreement with the experimentally measured casing velocity using the ultra-high-speed camera. Additionally, velocity values up to 3,805 m/s are obtained at the casing's tip. This corresponds to a 25 percent higher velocity at the casing tip than in the transverse direction. Figure 11 shows the total energy-time plot for the aluminum casing in contact with the PETN base charge.

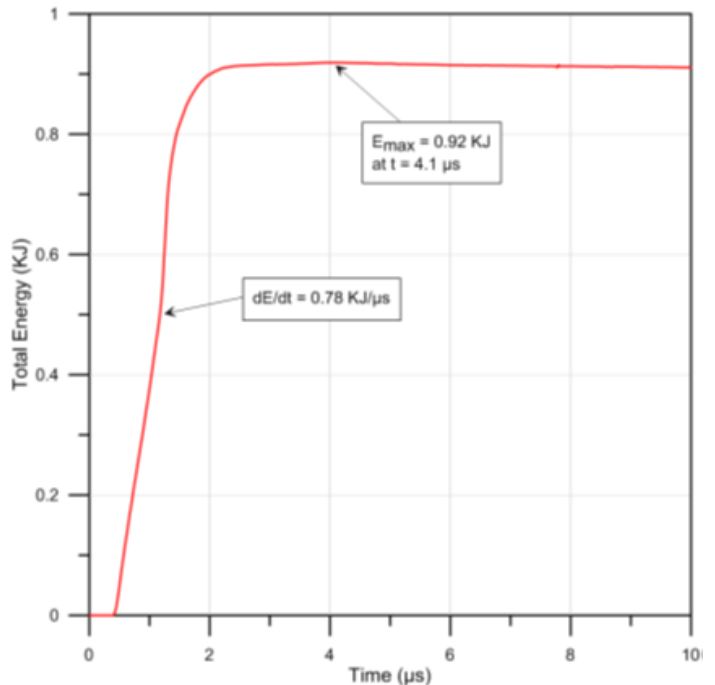
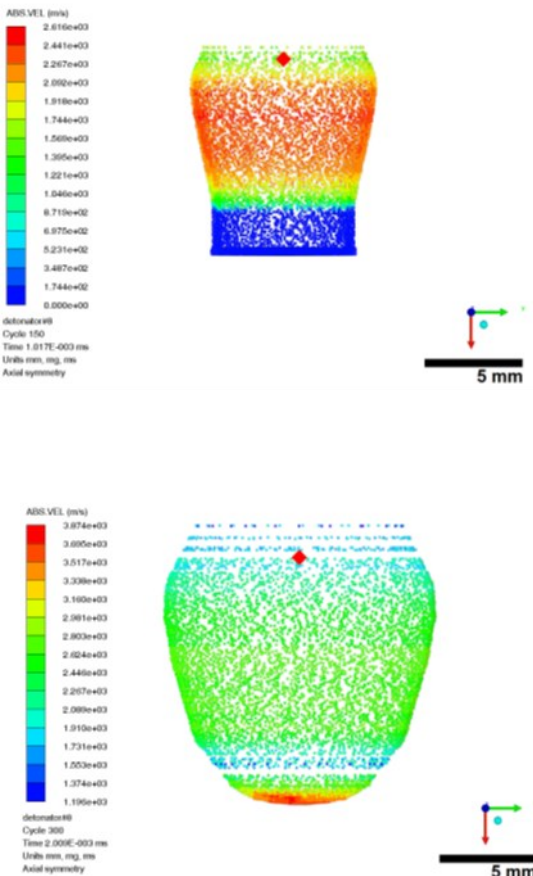


Figure 11. Total energy versus time (AUTODYN 2-D)

According to Figure 11, the detonation products transmit the energy to the casing at a rate of $0.78 \text{ KJ}/\mu\text{s}$ during the initial stages of the detonation. The energy of the aluminum reaches a peak of 0.92 Kilojoules at $4.1 \mu\text{s}$ after the initiation of the PETN charge. After that, the detonation products stop the energy transfer to the casing and the primary fragmentation would start to slow down due to the drag imposed by the medium. The model does not consider any medium surrounding the charge; therefore, the kinetic energy remains constant after the maximum is reached. A short interval of about $0.5 \mu\text{s}$ is observed in Figure 11 between the zero and the change in the curve slope. This is the time that it takes for the detonation front to reach the charge outer radius during the detonation process since the initiation takes place at a single point.

By comparing the energy values obtained from Equations (7), (8), and (10) and those obtained from the numerical simulation, it seems that Equation (10) is the one that better predicts the momentum absorption by the aluminum casing. This value is only 7.3 percent lower than the one obtained from the model. The difference is likely to be attributed to the energy absorbed by the detonator's tip. Murphy et.al. [21] analyzed a similar situation where the velocity of the high speed-flyer plate from a slapper detonator is measured using Schieleren imaging.

One last step in the characterization of the detonator is done by analyzing the size distribution of the fragmentation generated. A number 8 electric detonator is then detonated in a cylindrical aluminum container with a capacity of 3.8 liters. The container is filled with shock absorbing foam with dynamic viscosity of $1 \text{ KPa} \cdot \text{s}$. The main purpose of the foam is to absorb most of the kinetic energy of the fragments before they impact the container's walls. After detonation, the content of the aluminum cylinder is filtered through two metal sieves with openings corresponding to 1.81 mm and $850 \mu\text{m}$ (Figure 10). The fragments from the detonator's shell are then collected and digitally analyzed using ImageJ. ImageJ is an open source image processing program designed for scientific multi-dimensional images.

Fragments from the different parts of the detonator are dispersed in all directions. A wide variety of fragment sizes can be observed in Figure 12. However, those from the casing in contact with the base charge are of main interest (primary fragmentation). Some internal components, such as the bridge plug or the steel sleeve that houses the primer charge, can be also observed.

The particle analysis performed in Figure 12 revealed the fragment area distribution of the primary fragmentation. As it is shown in Figure 13, the majority of the primary fragmentation has an area ranging from 1 mm^2 to 12 mm^2 . The highest frequency is reached for fragment areas between 2 mm^2 and 3 mm^2 .

The fragmentation size distribution presented here is particularly interesting for the discretization of the detonator casing and the application of computational methods such as the smoothed-particle hydrodynamics (SPH) previously shown. Additionally, and in combination with the velocities obtained, it provides valuable

information for hazard evaluation in case of accidental detonation.

The fragmentation size distribution presented here is particularly interesting for the discretization of the detonator casing and the application of computational methods such as the smoothed-particle hydrodynamics (SPH) previously shown. Additionally, and in combination with the velocities obtained, it provides valuable information for hazard evaluation in case of accidental detonation.

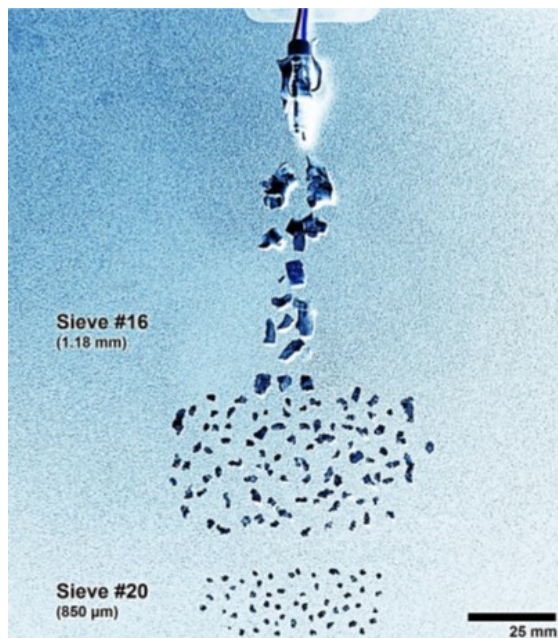


Figure 12. Fragments recovered from the detonator (negative image) and digital particle size analysis

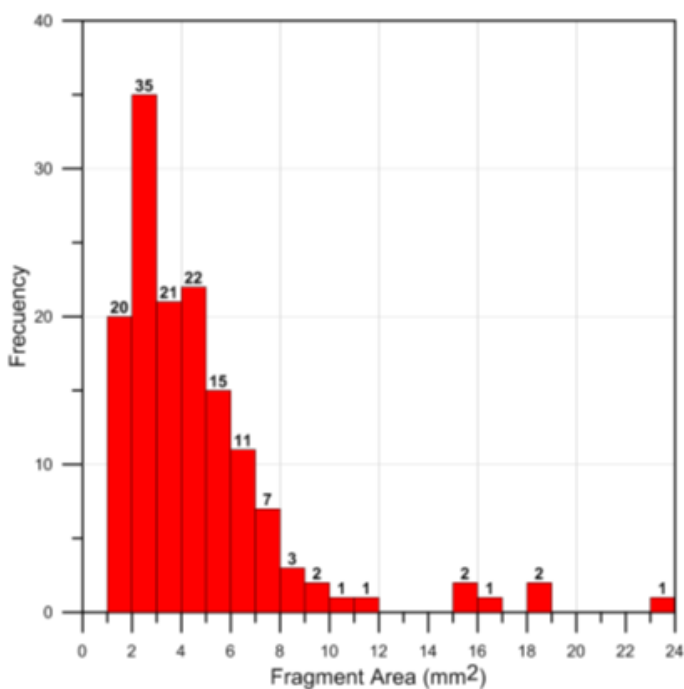


Figure 13. Fragment area histogram of primary fragmentation

4.5. Explosive Energy Partition

The total energy released by the detonation can be obtained by multiplying the explosive masses of the primer and base charges by their heat of detonation. However, since the primer charge is housed in a heavy steel casing and has a very low heat of detonation – about 25 percent of the heat of detonation of the PETN – its contribution to the final shock output could be considered negligible. This assumption is evaluated by using the Hutchinson equation since Fisher's formula fails for $M/C > 5$ [6]. The steel sleeve has a total mass of 7,769 mg while the associated section of the shell is 980.42 mg of aluminum. For the 330 mg of primer charge, this corresponds to an M/C equal to 26.51. By applying Equation (9), the resultant mass of equivalent bare charge is 47.59 mg.

This result implies that 86.4 percent of the explosive energy is absorbed by the casing and the sleeve. The rest is used to initiate the base charge and has a negligible effect on the generation of the primary blast wave and primary fragmentation. A similar argument could be made for the electrical energy that is applied to the bridgewire. This energy usually ranges from 5 to 10 mJ for standard electric detonators [20], which means that the electrical energy is 5 orders of magnitude lower than the energy coming from the explosive base charge. Figure 14 summarizes graphically the explosive energy partition for a standard number 8 electric detonator. The column on the left hand side shows the explosive energy value derived from the heat of detonation and the mass of explosives reported by the manufacturer. The column on the right hand side shows the energy partition obtained by the experimental and numerical methods.

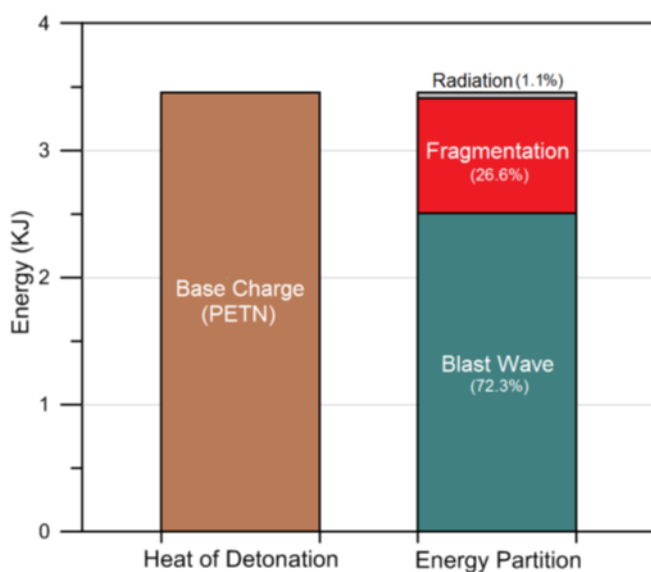


Figure 14. Explosive energy contained and released by a number 8 electric detonator.

Figure 14 shows that 98.9 percent of the entire energy

set free by the detonation is converted into the generation and rapid expansion of the detonation products, the driving mechanism for the blast wave and the fragmentation. About a quarter of the total chemical energy is in the fragmentation process while the rest goes to the blast wave formation. Only a 1.1 percent remains left that is likely attributed to the radiation emitted in the chemical reaction.

5. Conclusions

The retro-reflective shadowgraph technique has proven to be a fast and accurate tool for characterizing the strength of detonators compared to the traditional indirect methods. Additionally, it allows for the study of different modes in which the chemical energy is converted and how it is distributed. A total of 9 electric detonators were tested using high-speed and ultra-high-speed imaging techniques. By measuring the shock wave expansion rate, the primary blast wave in the air is characterized. Shock wave parameters are successfully calculated versus distance and time scales. Optical measurements were additionally validated using piezoelectric pressure gauges that recorded overpressure versus time histories at specific locations.

Because of their geometry, standard detonators show an initial ellipsoidal shock expansion that degenerates into a final spherical wave. This non-uniform shape creates variable blast parameters along the primary blast wave. For this reason, transverse and longitudinal directions are studied and the equivalent geometric sphere is calculated. From the shock Mach number versus distance, a single blast yielding coefficient is obtained within a 5 percent difference using the high explosive blast standard. A total energy of 2.5 KJ is then assessed to the shock load.

Finally, the energy fraction spent in the fragmentation process of the aluminum casing is obtained using the Gurney model. Three additional empirical formulations are also presented and their results compared (Fisher, Modified Fisher, and Hutchinson). These formulations consider exclusively the fraction of the energy that is transmitted to the surrounding cylinder of casing. However, part of the explosive energy is exerted on the shell's tip, imparting high velocities to this small area. For this reason, a two dimensional numerical model is built in AUTODYN 2-D using the SHP solver. The results from the numerical simulation account for that fraction of the energy, improving the overall analysis. A total energy of 0.92KJ is finally attributed to the fragmentation. In general, Hutchinson's equation provided the best results within an 8 percent range versus the other formulations. The fragment size distribution was also studied using particle imaging analysis, showing that the majority of the primary fragmentation has an area ranging from 1 mm² to 12 mm² with the highest frequency for fragment areas between 2 mm² and 3 mm².

Understanding the fragment density distribution plays a critical role when performing hazard evaluation from these types of devices. A final energy value of 3.42 KJ was obtained from the contributions of the shock and fragmentation. This value is only 1.1 percent lower than the chemical energy content of the PETN base charge (3.46 KJ). This difference is mainly attributed to the release of energy in the form of radiation. Additionally, it has been proven that the energy contribution from the primer detonator charge is negligible in relation to the

shock and primary fragmentation.

In general, this manuscript has shown a method to relate the strength of a detonator to a value of energy in Kilojoules. Understanding how the energy is released and in what quantities is critical for the performance evaluation of these devices. Future work will be performed by AXPRO at Colorado School of Mines for the characterization of the energy output for different types and strengths of commercial detonators using shadowgraph imaging.

Acknowledgements

We would like to thank the Colorado School of Mines Mining Engineering Department for the use of the Explosives Research Laboratory. We would also like to thank Jonathan Mace, from Los Alamos National Laboratory, for providing us with the knowledge and equipment to develop our shadowgraph research capabilities. As well, we would like to acknowledge the support of Vision Research, specifically Frank Mazella and Rick Robinson, for their encouragement of the advancement of our experimentation.

References

- [1] Bureau of Alcohol, Tobacco, Firearms and Explosives, "ATF Explosives Industry Newsletter", United States Department of Justice, December 2014, <https://www.atf.gov/file/21986/download>.
- [2] Environmental Protection Agency, AP 42, Fifth Edition, Volume I, Chapter 15: Ordnance Detonation, 15.9: Blasting Caps, Demolition Charges, and Detonators. https://www3.epa.gov/ttnchie1/ap42/ch15/draft/d15s09_jul09.pdf
- [3] H.Kleine, J.M.Dewey, K.Obashi, T. Mizukaki, K.Takayama, "Studies of the TNT Equivalence of silver azide charges", Shock Waves (2003) 13:123-138.
- [4] M. J. Hargather and G. S. Settles, Optical measurement and scaling of blasts from gram-range explosive charges, Shock Waves 2007, 17, 215-223.
- [5] M.M.Biss, "Energetic Material Detonation Characterization: A laboratory –scale Approach", Propellants, explosives, and pyrotechnics, 38, 477-485, 2013.
- [6] M.D.Hutchinson, "The escape of blast from fragmenting munitions casings", International Journal of Impact Engineering, 36, 185-192, 2009.
- [7] G.F. Kinney, K.J.Graham, "Explosive Shocks in Air", Second Edition, 1985.
- [8] C..E. Needham, "Blast Waves", Shock Wave and High Pressure Phenomena, DOI 10.1007/978-3-642-05288-0, Springer, 2010.
- [9] P.W. Cooper, "Comments on TNT Equivalence", Sandia National Laboratories, 20th International Pyrotechnics Seminal, July 14-29, 1994.
- [10] E.D. Esparza, "Spherical Equivalency of Cylindrical Charges in Free-Air", Southwest Research Institute, 25th Department of Defense Explosives Safety Seminar, 1992.
- [11] J. M. Dewey, Air velocity in blast waves from TNT explosions, Royal Society of London Proceedings Series A 1964, 279, 366-385.
- [12] Kingery C. N., Bulmash G., (1984) "Technical report ARBRL -TR-02555: Air blast parameters from TNT spherical air burst and hemispherical burst", AD-B082 713, U.S. Army Ballistic Research Laboratory, Aberdeen Proving Ground, MD.
- [13] G. I. Taylor. The formation of a blast wave by a very intense explosion .1. Theoretical discussion. Proceedings of the Royal Society of London Series A-Mathematical and Physical Sciences, 201(1065):159–174, 1950.
- [14] M. J. Hargather, "Scaling, characterization, and application of gram-range explosive charges to blast testing of materials", Pennsylvania State University, 2008.
- [15] G.W.Gurney, "The initial velocities of fragments from bombs, shells, and grenades", Ballistics Research Laboratories, Report 405, 1943.
- [16] Dyno Nobel, *Electric Super™ SP* Technical Information, <https://goo.gl/XF01ci>
- [17] M.J. Hargather, G.S. Settles, "Retroreflective shadowgraph technique for large-scale visualization", Applied Optics, 2009, 4449-4457.
- [18] S. E. Rigby, A. Tyas, S. D. Fay, S. D. Clarke, J. A. Warren, "Validation of semi-empirical blast pressure predictions for far field explosions – is there inherent variability in blast wave parameters", 6th International Conference on Protection of Structures against Hazards 16-17, Tianjin, China, October 2014.
- [19] R. Weinheimer, "Properties of selected high explosives", Los Alamos National Laboratory, 27th International Pyrotechnics Seminar, 16 – 21 July 2000.
- [20] P.W. Cooper, "Explosives Engineering", ISBN 0-471-18636-8, 1966.
- [21] M.J. Murphy, R.J. Adrian, "Particle response to shock waves in solid: dynamic witness plate/PIV method for detonations", Experiments in Fluids, 2007, 43, 163-171.

Danish experiences with obtaining regulatory approval for explosives storage facilities

C. A. Andersen, S. Qvist, K. C. Jørgensen
NIRAS A/S, Allerød, Denmark

ABSTRACT: In 2008 Denmark introduced new legislation regarding the commercial use of explosives. The legislation introduced new requirements to explosives storage facilities, including specifying safety distances to various types of objects like schools, hospitals, major roads and housing. The safety distances are based on the *AASTP-1 Manual of NATO Safety Principles for Storage of Military Ammunition and Explosives* and its guidelines for storage of more than 500 kg NEQ, but are applied to all storage of more than 0.5 kg NEQ.

The legislation poses a challenge to users of explosives as Denmark is a fairly densely populated and urbanised country without large tracts of undeveloped land and therefore there are practically no areas that meet the safety distance to roads or housing. This, combined with the fact that permits given under the previous legislation were usually valid for 5 years, has led many Danish users of explosives into a limbo in recent years, where permits for storage of explosives expired but no new permits could be given.

The legislation however allows for exemption from the safety distances if a risk analysis deems the storage facility safe. Usually risk is defined as likelihood multiplied by consequence but this alone does not solve the problem, as there are no risk acceptance criteria set.

Currently the only solution is to design new explosive storage facilities in such a way that the facility itself will contain or mitigate the consequences of an accidental explosion, to a level where the consequences at nearby objects will be less than if the safety distances had been met.

Some of the possible parameters that affect the projection of consequences include the NEQ, orientation, size, ventilation areas and possible burial of the facility, along with earthworks and terrain features between the facility and the object in question.

Up to now, half a dozen storage facilities have been approved using this method.

Recently, the Danish Emergency Management Agency (DEMA) has proposed risk acceptance criteria, giving the possibility to include likelihoods in the risk analysis. The criteria are pending approval by the Danish Ministry for Justice and so far no storage facilities in Denmark have been approved based on this.

1. INTRODUCTION

Denmark is generally a flat country with an underground consisting of gravel and clay. Apart from the small island of Bornholm, the bedrock is far below the surface and therefore the use of explosives is generally less common than in some of the neighbouring countries.

The main civilian use of explosives in Denmark is in the construction industry for cutting concrete piles, removing unwanted concrete, demolition or landscaping.

This leads to a relatively low number of civilian users of explosives, spread around the country and to a relatively low knowledge of the properties of explosives amongst the authorities and population in general.

2. LEGISLATION

The current Danish legislation on the civilian storage of explosives are given in the *Administrative Order on Explosive Materials (Bekendtgørelse om eksplosivstoffer) BEK 1247 of 30 October 2013*.

For the storage of more than 500 g of regular explosives (Hazard Division 1.1), the relevant requirements are given in

Table 1.

Table 1. Requirements for the storage of more than 500 g of HD 1.1 explosives in Denmark. Excerpt from BEK 1247.

| Article | Requirement |
|---------|---|
| 5.1 | Police approval |
| 5.2 | Storage must be inaccessible to third parties |
| 5.3 | Stored articles must not be subjected to impact, friction, heat etc. |
| 5.4 | Storage may not be in the same building as dwellings |
| 5.6 | Stored articles must be kept in the original packaging |
| 7.1.2 | Safety distances must be observed, See Table 2 |
| 7.1.3 | Storage must be in a cast (concrete) vault or in a safe |
| 7.1.4 | Vault or safe must be locked at all times |
| 7.1.5 | Storage facility must have an automatic burglar alarm |
| 7.1.6 | The storage facility may not be used for storing other items |
| 7.1.7 | Compatibility groups must be observed |
| 7.1.10 | Signage: Danger, Explosives, No smoking etc. |
| 7.1.11 | Firefighting equipment must be present |
| 14.1 | The police can under certain circumstances grant an exemption from the regulations in Article 7 |
| 14.2 | Exemption from the safety distances in Article 7.1.2 requires the applicant to submit a risk analysis that shows that the storage facility is safe. The police submits the risk analysis to the Danish Emergency Management Agency for approval |

The safety distances referred to in article 7.1.2 are based on *AASTP-1 Manual of NATO Safety Principles for the Storage of Military Ammunition and Explosives* and are calculated using the formula

$$D = k \cdot Q^n \quad (1)$$

where D is the safety distance and Q is the quantity of explosives. k and n depend on the nearby object in question and are shown in Table 2.

Table 2. Safety distances for the storage of more than 500 g of HD 1.1 explosives in Denmark. Excerpt from BEK 1247.

| No | Object | Calculation parameters | Minimum safety distance |
|----|--|-----------------------------|----------------------------|
| 1 | Hospitals, schools, kindergartens, tall buildings and similar | $k = 44,4, n = \frac{1}{3}$ | $D_{\min} = 800 \text{ m}$ |
| 2 | Dwellings | $k = 22,2, n = \frac{1}{3}$ | $D_{\min} = 400 \text{ m}$ |
| 3 | Buildings and other activities not related to the storage facility, cf. row 1 and 2. | $k = 22,2, n = \frac{1}{3}$ | $D_{\min} = 270 \text{ m}$ |
| 4 | Public roads, ports, railroads and similar without constant dense traffic | $k = 14,8, n = \frac{1}{3}$ | $D_{\min} = 180 \text{ m}$ |
| 5 | Public roads, ports, railroads and similar with constant dense traffic | $k = 22,2, n = \frac{1}{3}$ | $D_{\min} = 270 \text{ m}$ |
| 6 | Occupied buildings within the same site as the storage facility | $k = 22,2, n = \frac{1}{3}$ | $D_{\min} = 270 \text{ m}$ |
| 7 | Other storages of explosives without traverse protection | $k = 22,2, n = \frac{1}{3}$ | $D_{\min} = 90 \text{ m}$ |
| 8 | Other storages of explosives without traverse protection | $k = 2,4, n = \frac{1}{3}$ | $D_{\min} = 9 \text{ m}$ |

3. APPROVAL PROCEDURE

Before an explosives storage facility can be built, a regulatory approval must be obtained. The applicant must submit an application to the police, containing plans for the storage facility, specifying the location and intended amount of explosives to be stored.

The police will then forward the application to the Danish Emergency Management Agency (DEMA) for commenting. DEMA will then check whether the regulations, including the safety distances are observed and issue recommendations to the police on whether to approve or reject the application. The police will then inform the applicant of the decision.

In cases where the safety distances are observed, this process is relatively easy and straight-forward.

The challenge is that Denmark is a highly urbanised and relatively densely populated country with a population density of ~130 per km² and a developed road network. Therefore it is almost impossible to find any areas where the safety distances to dwellings and roads can be observed. Consequently, all applicants have to ask for exemption under Article 14.2 of BEK 1247 and produce a risk analysis showing that the site is safe.

3.1. Risk analysis

In general risk is defined as shown in Equation 2.

$$\text{Risk} = \text{Probability} \cdot \text{Consequence} \quad (2)$$

Risk is often expressed in terms of the expected number of fatalities per year. A standard method for conducting a risk assessment is to estimate the probabilities and consequences of the adverse events and compare the product thereof to a set threshold value or acceptance criteria. This method is for instance used for risk assessments for sites containing dangerous substances in accordance with Directive 2012/18/EU (the Seveso III Directive).

The challenge is that in the current Danish regulations, there are no set acceptance criteria, a criteria that can be administratively defined by the Danish Ministry for Justice.

Therefore, a slightly different approach is needed, where it is assumed that an explosion of the largest possible magnitude will definitely take place (probability set to 1) and then designing the storage facility in a way that ensures that the consequences (overpressure) at any nearby object will be equal to or less than if the safety distances of BEK 1247 had been observed.

4. DESIGN OF STORAGE FACILITIES

There are six parameters that influence the magnitude of the pressure at a certain distance from an accidental explosion in an explosives storage facility. They are:

- Charge weight [kg]
- Stand-off distance [m]
- Room volume [m³]
- Vent area (door) [m²]
- Orientation in relation to the storage facility [front, side, rear]
- Interlaying terrain [-]

For a planned explosives storage facility, all of the nearby objects mentioned in Table 2 must be identified and the overpressure at each object must be determined and shown to be lower than if the safety distances of BEK 1247 had been observed.

The American Defence manual UFC 3-340-02 Structures to Resist the Effects of Accidental Explosions (formerly known as TM 5-1300) provides graphs of the relationship between pressure, scaled distance and scaled venting to the front, side or rear of a partially vented four-wall cubicle. Scaled distance is defined as seen in Equation 3.

$$Z = \frac{R}{W^{\frac{1}{3}}} \quad (3)$$

where Z is the scaled distance, R is the stand-off distance and W is the charge weight.

Scaled venting is defined as seen in Equation 4.

$$A_{v,s} = \frac{A}{V^{\frac{2}{3}}} \quad (4)$$

where $A_{v,s}$ is the scaled venting, A is the venting area and V is the room volume.

The NATO manual AASTP-1 Manual of NATO Safety Principles for the Storage of Military Ammunition and Explosives provides guidelines to whether an object should be considered to be in front, to the side or rear of the storage facility.

The above relations are then used to determine a set of related values for the room volume, vent area, allowable charge weight and facility orientation, that will produce tolerable pressures at all nearby objects. This is an iterative process that is not easily automated.

4.1. Terrain

The method presented above is generally valid for flat open terrain. Any permanent terrain features present between the explosives storage facility and a nearby object can be taken into account, say if there is a hill between the storage facility and an object.

4.2. Fragments

The legislation specifies minimum distances (see Table 2) due to possible fragments. As the civilian use of explosives rarely includes cased explosives like grenades, only secondary fragments from the storage facility are considered.

If the storage facility is built as a buried structure with an earth cover and the cover is free from rocks or stones, it is possible to neglect the minimum distances. AASTP-1 also specifies minimum criteria for cover thickness.

4.3.Other considerations

Apart from the safety distances, the storage facility must also be designed to meet a number of other criteria with regard to:

- General construction standards and codes (Eurocode)
- Ventilation
- Indoor climate (temperature, humidity)
- Burglary prevention and alarms
- Fire safety
- Lightning conduction
- Etc.

5.OUTLOOK

The current practice only includes the consequence aspect of the risk analysis. Therefore all the explosives storage facilities designed using this method are several orders of magnitude safer than they might have to be. DEMA is aware of this and work is currently ongoing to define risk based criteria, that will also allow the probability of an explosion to be taken into account in the risk analysis.

DEMA has proposed risk based criteria as shown in Table 3.

Table 3. Risk based acceptance criteria proposed by DEMA.

| | Acceptance criteria |
|---|--|
| Individual risk | |
| Persons directly involved in work with explosives | Rules for general labour safety (Rules set forth by the Danish Working Environment Authority) |
| Other persons employed in the same business | 10 ⁻⁵ per year |
| Third person | 10 ⁻⁶ per year |
| Risk to society | A curve of accumulated frequencies where the frequency for 1 death is 10 ⁻⁴ per year and which decreases in relation to the square of the number of deaths. The frequency for 1,000 deaths must be 0. |

Formally the risk criteria must be issued by the Danish Ministry for Justice, so DEMA’s proposed criteria have not yet been approved but work is already ongoing for at least one company to submit an application for approval based on the risk

5.CONCLUSIONS

Since the implementation of the Administrative Order on Explosive Materials in 2008, civilian users of explosives have had difficulty in obtaining the required permits and approval to store explosive materials.

The legislation provides safety distances between explosives storage facilities and nearby objects, that cannot be kept in practice. Therefore users must provide a risk analysis that shows that the facility is safe. The legislation is very conservative, as it only considers the potential consequences of an accidental explosion and does not allow for the probability of occurrence to be taken into account.

ties in such a way that the facility itself will contain or mitigate the consequences of an accidental explosion, to a level where the consequences at nearby objects will be less than if the safety distances had been met, has been developed and implemented. Currently, half a dozen explosives storage facilities have been approved using this method.

A process has been started by DEMA to allow the probability of occurrence to be taken into account. Work is ongoing to get the first approval based on this method, but the proposed risk criteria have yet to be confirmed.

A new risk based method will reduce the overall cost of construction because facilities could be placed closer to other objects and would not have to be as sturdy as before. Even though the cost of the risk analysis would be higher, the overall cost will be lower.

REFERENCES

1. Danish Ministry for Justice, 2013, Administrative

Therefore a practice of designing explosive storage facilities. While SAFEX International selects the authors of articles in this Newsletter with care, the views expressed are those of the authors and do not necessarily represent the official position of SAFEX International. Furthermore, the authors and SAFEX International cannot accept any liability for consequences arising (whether directly or indirectly) from the use of any advice given or opinions expressed in this Newsletter

Order on Explosive Materials (Bekendtgørelse om eksplosivstoffer) BEK 1247 of 30 October 2013 incl. addenda and corrigenda

2. United States Department of Defence, 2008, UFC 3-340-02 Structures to Resist the Effects of Accidental Explosions, Change 2, September 2014.
3. NATO, 2006, AASTP-1 Manual of NATO Safety Principles for the Storage of Military Ammunition and Explosives.
4. EU, 2012, Directive 2012/18/EU on the control of major-accident hazards involving dangerous substances, amending and subsequently repealing Council Directive 96/82/EC, July, 2012.

best employed during informal karaoke sessions or serious speechifying. Look it up on 'You Tube' to see a performance. For best results, simply place the hat upon your head and position oneself behind the person singing or giving the speech. Keep your face straight and activate the hat's hidden mechanism. The hat will do all that is required.



Other signs of an impending Christmas include fairy lights, sleigh bells, mistletoe (must buy that denture fixative right away) and lots of Ho, Ho, Ho and a bottle of rum.

THE LAST POST

By

Anthony Rowe

A bugle call signifying the lowering of the flag at the end of a day's activities. Also used at funerals and

military ceremonies

Forgive me if I have mentioned this before, but I am old. I am so old that even my dandruff has antique value. My mental age, however, seems stable. In my mind I am still about 23 years old, but when I look in a mirror I'm amazed to see a wrinkly-faced old geriatric staring back. He seems harmless enough, but his face looks like it has been unfolded and refolded too many times. He wears bottle-bottom spectacles, has fur lined ears, bushy eyebrows and hairy nostrils, but not a single hair on his head or chest.

The years have clearly not been kind.

Another looming and clearly relevant problem is that I can no longer remember what I have written and, as I don't save or keep my musings there remains a clear and present danger of repetition. I perceive therefore that my literary career is fast coming to a close. I seem to recollect that the year is 2016, but can't be sure. You see I no longer wear a watch, use a cellphone or watch TV. I think I have become a hermit.

Since the winds and rain appear to have abated, the holiday traffic is increasing, I suspect Christmas will soon be upon us. Confirmation seems to be provided by the sudden unearthing - by my daughter no less - of my famous dancing Santa hat. This item of apparel is

Speaking of rum, wasn't Admiral Horatio Nelson's body kept pickled in a barrel of rum or possibly brandy following his death by sniper fire at the Battle of Trafalgar in 1805? Legend says that the sailors subsequently bored holes in the cask and sucked out the raw spirit using straws in a process called "tapping the monkey." I think the tale is just a myth, but the story perhaps explains why the daily rum ration issued to British sailors became known as Nelson's Blood. The rum ration itself was finally abolished in 1970. (*The Royal Navy hasn't been quite the same since*).

Trafalgar itself lies just a few kilometers south of my present location in South Africa, but just between you and me, I don't think it's the right place. I've looked and looked, but I can't find any bits of ships rigging or cannonballs anywhere. I did find the odd Portuguese Man of War. These were small, but still well armed, but the ships I was on the lookout for were predominately either French or English. I did, however, find an empty bottle of a well-known French brandy plus a pair of ragged old underpants identifiable as English by their sewn-in 'St Michael' label and Union Flag motif. I am amazed by the stitching skills of those seamstresses back in 1805. I also found some chunks of lead carefully camouflaged as fishing weights. Maybe Nelson was actually shot with a fishing weight? Could be? Who is to say that the sniper wasn't a keen fisherman who simply mixed up his bullets with his fishing gear?

All that said, we are supposed to talk safety, so noses to the fly-wheel and let's get on with it.

Everybody knows that once initiated, explosives explode, but that's not always true. Sometimes they don't. A shot or pyrotechnic event that has been initiated, but subsequently failed to explode or burn is called a misfire and every misfire is an accident waiting to happen. There are a host of potential causes for misfires and these include both manufacturing and end user er-

rors. A small percentage can result from faulty assembly, poor soldering, (possibly creating intermittents) incorrect pressing pressures or fusehead damage. Field failures can also occur from mechanical abuse such as driving over wires or connections or even the ingress of aggressive or electrically conductive liquids.

Whatever the cause, prevention is better than the cure. It is always to the end users advantage to spend more time engaged in pre-blast prophylaxis than the more hazardous post-blast process of remediation.

This situation, often created by a detonator that has failed to respond, can be an extremely hazardous one. If it is just a detonator with no additional explosives present the problem is probably addressable by a trained operator at relatively low risk, but in general the more explosives there are attached to that detonator, the higher the risk. All well and good, but it's the actions that you take to resolve the issue that may directly influence your life expectancy.

Let's consider one safety issue, the problem of the safe removal of a misfired (reverse primed) detonator and the possibility of stress cracking of the initiating medium (shocktube/fuse etc.) at the bend. Hole diameter will be an influencing factor in this regard. The narrower the hole diameter the more difficult it will be to remove a misfired detonator that has been reverse primed. There is also the issue of damaging the fuse or shocktube during its insertion into the hole and by doing so creating the very misfire that must now be addressed. Assemblies bent back upon themselves are difficult not only to remove, but also to insert. Charging up therefore may require the use of a tool of some sort. The tools available at the face (Pinch bar, drill steel, charging lance etc.) may be less than ideal and their use as insertion aids can raise serious safety issues.

Speaking of fuse and despite a long and distinguished history of more than 50 years of million a day sales, the long obsolescent connector capped fuse and ignitercord system, had its shortcomings. Although extremely rare, safety fuse could apparently stop burning, appearing in all aspects to have gone out, but the sneaky little blaster could still be smoldering internally. Technically speaking such events are more correctly called 'hangfires.' What makes them potentially lethal is that an affected fuse can suddenly and miraculously re-light and in the wink of an eye resume normal burning once again. Not much fun when you are only 5 meters away from a potential shotgun blast of broken rock.

In retrospect, we now know that the use of cotton yarns in the semifuse is more likely to create this phenomenon

than the use of jute. Why? Well it's a property of cotton to smolder aggressively.

The later introduction of a slower burning variant of safety fuse also presented difficulties for the untrained or unaware. The original product would burn at around 2 minutes a meter, (actually 99 – 121 sec/meter) but its slower burning counterpart, burned at ca 5 minutes a meter (actually 260 – 320 sec/meter).

You needed to have your wits about you when you engaged in secondary blasting. An unwary or inexperienced operator, perhaps mixing up his fuses, might assume a misfire and could walk into a bang. A difference of ca 3 minutes per meter is a long time when you are waiting for something to happen. Best to know the burning rates of the fuses you are using. If you are unsure, walk slowly my friend. Walk very, very slowly. Limp a bit. Better still, limp a lot.

The remedy for both complaints is time. If nothing happens when it is supposed to, simply wait. Wait at least sixty minutes before going to investigate and don't just guess the time, use your watch! Short cuts here can mean a serious reduction in lifespan.

By the same token do avoid using capped fuse products in blasting operations where third parties can gain access to the blasting site. Once lit, fuse will normally burn to completion. It will then initiate its attached detonator and shortly thereafter, the bulk explosives. The user has no control whatsoever and no knowledge of exactly when the shot will go off. Should somebody – following successful fuse ignition – gain access to the site, Santa's sleigh touchdown, a helicopter hover overhead or a busload of girls in swimwear crash through the barriers, the shot or shots will still go off. The blast cannot be safely aborted.

How much better to use an either an instantaneous or No. 0 electric detonator? Should circumstances or conditions suddenly change - even up to the last second, the key need not be turned or the firing switch depressed. You keep control and both Santa and his reindeer stay safe, not to mention all those girls on the bus.

Fuse can actually burn faster than advertised. This happens when the fuse covering is prevented from melting and the gases generated by combustion are unable to escape. Pressures within the fuse rise and the burning rate increases.

Misfires in a stope, development end or raise cause additional problems. Even though the area is probably safe to approach, (the shots usually having been initiated hours earlier) the misfired detonator and the column of explosives that surround it may have to be removed before drilling can commence and the next blast be connected up. This relatively simple process has killed and injured many persons over the years.

Few, if any end users still employ the impact sensitive NG-based explosives like Dynamite Dynagel and Gelignite. These powerful

blasting explosives have been replaced with the relatively impact insensitive ANFO's, emulsions or watergels. Ammonium nitrate, (AN) on its own is especially difficult to detonate, although, where you have ammonium nitrate in the form of an ANFO (ammonium nitrate and fuel oil) – its initiation by impact is theoretically possible, but not probable as the mixture still remains relatively insensitive. The most likely mechanism of initiation would be a detonator. Detonators are impact sensitive and the initiation of such a device under confinement in the presence of an ANFO would almost certainly lead to the initiation and propagation of the bulk explosive.

Black powder or blasting gunpowder is also impact sensitive. It generally kills its victims by burning.

Detonators are amazingly robust little critters, but only as long as their protective metal shell remains intact. Break, tear or rupture the shell and what is inside, can get outside. This is not good. You see what's pressed within is not friendly stuff, neither does it like being poked with anything, especially something as aggressive as a 'lance'. When disturbed it has only one defense. Technically it's called the Detonation Prerogative.

That's not actually true. I made it up, but I've got to admit it sounds pretty good.

In an instant following initiation the reaction accelerates from dead stop to a few thousand meters per second. This results in a shock and pressure wave followed by shrapnel. This apparent call to arms rallies the troops who may still surround it. Unresponsive thus far, but with their blood now up, they join in too. Charge !!!..... Their battle cries also sound a lot like **BANGI**, but only because we don't speak their tongue. However, it's now far too late to do anything to stop it. What must be, will be.

The same applies to a detonator struck by the cutting head or shaft of a working rock drill. The impact forces created by such an encounter are enormous and almost certain to cause the immediate initiation of any detonator struck in this way. This can happen when operations such as drilling and charging are taking place simultaneously. For such a thing to occur constitutes a major malpractice. In long holes (greater than 3 meters) the slightest deviation can result in the hole currently being drilled intersecting with an already drilled, but due to the malpractice, a now explosively primed and charged hole. If the drill now strikes the detonator in the newly charged hole, things can turn very ugly very quickly.

The drill steel itself is hollow and possesses a carborun-

dum (silicon or tungsten carbide) impregnated tip. The carbides are very hard and make good abrasives whilst the underlying purpose of the central passage is to provide a means of introducing cooling water or mixtures of air and water injected under pressure into the drill hole. This is done to both cool and flush rock cuttings away from the cutting head. A third and important function of the water in underground operations is the suppression of dust.

Anything which causes a blockage within the central water channel presents serious safety issues. It can restrict or completely cut off the flow of water to the drill tip. The result might be 'dry drilling'. This can result in heat build-up and reduced drilling efficiency combined with increased wear and tear on the drill bit. Should such a blocked up length of drill steel enter a hole containing a water soluble explosive like ANFO, there would be little or no water flow available to dissolve and desensitise any explosive material which might be present. Any explosive material residing within such a hole might be compacted, but not initiated. The presence of an undetonated downhole detonator perhaps concealed within the explosives column would change that. Should such a detonator be struck by the advancing drill tip it would almost certainly initiate. Any remaining explosive might also initiate and propagate. The result would be an explosion, which I am sad to say, generally has unfortunate outcomes for the drilling crew.

As well as being old I am also a poor man, some say a cheap-skate having short arms and deep pockets. Other maintain that I can bring out a cigarette already lit, but despite these shortcomings I still derive no small measure of pleasure and warmth as I take this opportunity to wish everybody in our industry a very happy Christmas. So, to all of you out there, from the most humble and lowest paid to the biggest of the big bosses, "May you gather your family around you and enjoy a truly wonderful Christmas!" Stay safe, stay close and wherever we are let's see in the New Year together.

It's your round by the way.

This may be my last article, but as usual, any technical errors are mine alone. With that all said and despite my nagging doubts, somewhat dubious historical knowledge, weak geography and fast developing senility let our New Years' Resolution be to make 2017 be the safest year ever.

If this could be achieved it would make an old man very, very happy.



SAFEX BOARD OF GOVERNORS

Chairman: John Rathbun (Austin International)

Governors: Andrea Sánchez Krellenberg (MAXAM);
 Claude Modoux (Poudrerie d'Aubonne);
 Andy Begg (Individual Associate);
 Terry Bridgewater (Chemring Group);
 Aleksandr Chernilovskiy (Azot Vzryv);
 Mike Powell (incitec Pivot);
 Rahul Guha (Solar Industries);
 Thierry Rouse (Groupe EPC);
 Edmundo Jimenez (ENAEX);
 Noel Hsu (Orica);
 Colin Wilson (AELMS)

ARTICLES FOR NEWSLETTER

This is a reminder that through the Newsletters we share knowledge in the areas of Safety, Health, Environment and Security pertaining to the Explosives Industry. SAFEX thus call on all members to submit articles on these subjects within their own companies and countries. **The deadline for articles for the March Newsletter is 30 February 2017 and I look forward to your support .**

SAFEX thanks the following authors for their invaluable support:

- John Rathbun ,Chairman , SAFEX International
- Dr SK (Jim) Chan, Expert Panel
- Dr Valentine A. Nzengung ,Munirem Evironmental
- Dr Jackson Shaver, Special Devices
- C. A. Andersen, S. Qvist, K. C. Jørgensen ,NIRAS A/S, Allerød, Denmark
- Tony Rowe , Retired AELMS.



The SAFEX International Board of Governors wishes each and every member ,company and industry friend a very enjoyable and Happy Festive Season and may 2017 be a safe and prosperous year for the SAFEX community

